

1

Supramolecular Graphene Nanocomposites and Applications for Chemo- and Biosensors

Gunnar Olsen, Arnab Halder and Qijin Chi*

Department of Chemistry, Technical University of Denmark, DK-2800 Kongens Lyngby, Denmark

*Corresponding author

Outline:

Introduction to graphene materials and their advantages	2
<i>Synthetic methods</i>	3
<i>Functionalization of graphene materials</i>	8
<i>Structural characterization</i>	12
Graphene functionalized with supramolecular moieties for Sensing	15
<i>Ionophore functionalized graphene for ion sensing</i>	17
<i>Cavitand functionalized graphene for neutral analytes</i>	18
<i>Turn-on fluorescence sensing by guest exchange of supramolecular functionalized graphene</i>	20
Biosensors based on supramolecular anchoring to graphene materials	23
<i>Enzymatic sensors</i>	24
<i>Non-enzymatic biosensors</i>	25
<i>Antibody and aptamer based biosensors</i>	26
Concluding remarks and outlook	27
References	28

Introduction to graphene materials and their advantages

Graphene is a single layer of a graphite crystal structure (Figure 1.1). Graphite was first discovered in Borrowdale about five centuries ago¹. It is a soft, mechanically weak and black material. Graphite was initially used for marking sheep. Its first formal use was driven by a military purpose as a heat resistant solid lubricant for canon ball molding². To date, graphite has been widely used in many practical applications from pencils to nuclear reactors². Before 2004, graphene as a free standing material was discussed and had been studied for more than 60 years, but its studies were limited to the theoretical level³⁻⁵. It was generally believed that graphene would not be stable enough to exist⁶⁻⁸. However, Novoselov, Geim and co-workers⁹⁻¹¹ demonstrated in 2004 that it is possible to mechanically exfoliate graphite using a scotch tape to obtain single layered graphene sheets, and graphene sheets are stable enough for experimental characterization. This pioneering work and following studies of its unique properties have led to a Nobel Prize in physics shared between Novoselov and Geim in 2010¹².

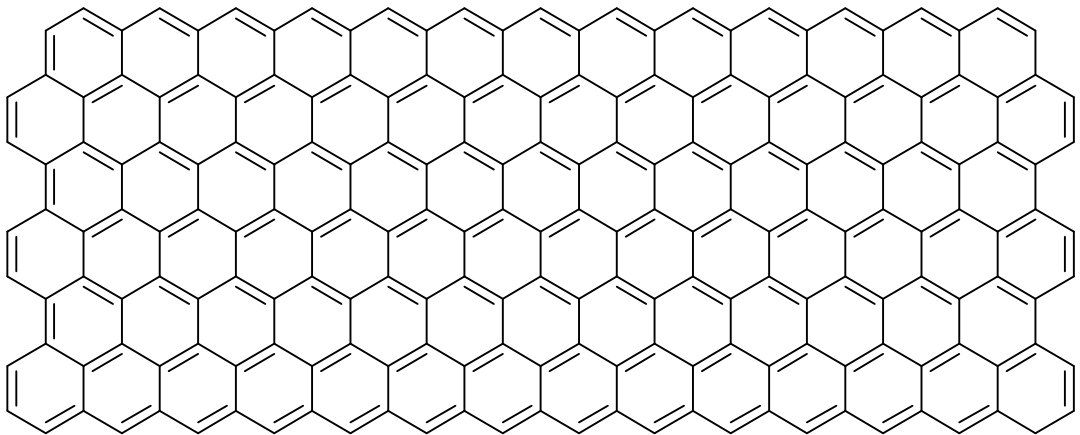


FIGURE 1.1

Chemical structure of pristine graphene, a hexagonal network of sp^2 carbon

The discovery by Novoselov and Geim *et al.* quickly started a new area of research, which has received tremendous attention in the scientific community. This has ever since grown rapidly, due to a series of experiments shortly after the discovery showing incredible electronic, optical, thermal and mechanical properties of this new material.

Graphene is an atomic flat two-dimensional crystalline material of sp^2 -hybridized carbon arranged in a hexagonal pattern with a bond length of 1.42 Å; each carbon atom covers an area of 5.25 Å².¹³ The highly conjugated π -system results in a highly delocalized electronic structure that gives rise to its remarkable electron mobility. Because graphene is an atomic flat material and can extend endlessly in two-dimensional geometry, the theoretical specific surface area is thus enormously high at 2630 m²/g twice as high as that for single walled nanotubes 1315 m²/g¹³. In fact, this value is higher than that of any other known materials. The optical properties of graphene has been reported and show that each layer of graphene only adds an opacity of $\approx 2.3\%$ and therefore graphene and few-layer graphene can be used in transparent devices¹⁴. The mechanical property was studied by AFM via nano-indentation on freestanding single layer graphene membranes suspended over holes on a Si substrate¹⁵. The experimental breaking strength and non-linear elastic

stress-strain were determined to calculate intrinsic strength and young's modulus of this material. Those experiments have confirmed that graphene is the strongest material ever discovered. Since graphite is considered to be brittle and mechanically weak, in this case, thickness thus plays a key role in determining mechanical strength. Thermal conductivity has been measured for both suspended graphene¹⁶ as $5000 \text{ W m}^{-1} \text{ K}^{-1}$ and graphene on a SiO_2 support¹⁷ as $600 \text{ W m}^{-1} \text{ K}^{-1}$, showing very high thermal conductivity.

Most impressive, however, are its electronic properties originating in the full conjugated 2D π -system. The electronic mobility in graphene on SiO_2 at room temperature has been reported by Novoselov *et. al.*⁹⁻¹¹ to be $\approx 2000\text{-}15000 \text{ cm}^2\text{V}^{-1}\text{s}^{-1}$ with charge carrier being tuned between electrons and holes at concentrations as high as $15\,000 \text{ cm}^{-2}\text{V}^{-1}\text{s}^{-1}$, even higher measurements have been carried out by Bolotin *et. al.*¹⁸ on suspended graphene extensively clean for impurities resulting in electron mobility of a staggering $230\,000 \text{ cm}^2\text{V}^{-1}\text{s}^{-1}$. Furthermore, graphene sheets exhibit a range of different quantum effects, including that due to the conjugated nature of π -electrons throughout graphene, these electrons can be described as massless Dirac fermions¹¹; ballistic transport of electrons on the sub-micrometer scale up to $\approx 0.3 \mu\text{m}$ at 300K ⁸, quantum hall effect at room temperature^{19,20} and zero energy band gap. It is noted that, however, all these unique properties are highly dependent on the quality of graphene sheets that must be truly single crystalline and do not have impurities or grain boundaries in sheets. In addition, they must be highly clean, and the experimental observations are affected by support materials as well.

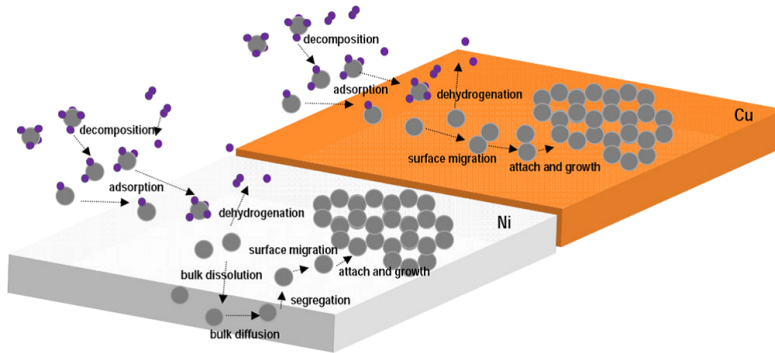
Synthetic methods

The first batch of graphene nanosheets was obtained by micro-mechanical exfoliation of graphite, which is also called the "scotch tape method". However, due to its scalability limitation of this method, other synthetic methods are needed and have been developed to produce graphene, some of which are outlined below.

Bottom-up growth of graphene

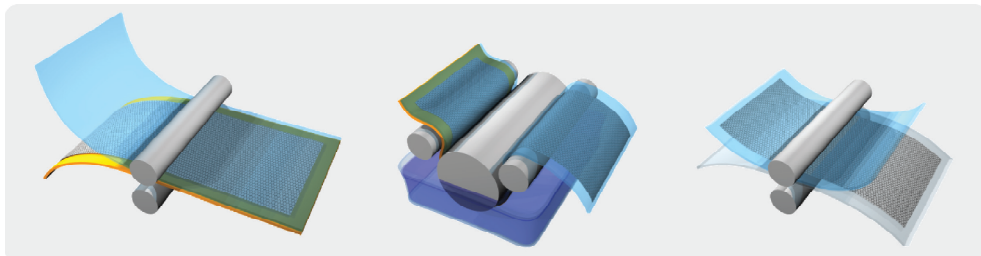
Bottom-up growing graphene represents one of the main alternative approaches to make high quality large-area graphene sheets. Growing graphene on a substrate can be done by two methods, i.e. chemical vapour deposition (CVD) and epitaxial growth on SiC. However, the latter is hardly considered as a facile way for large scale production, because this method needs atomically flat SiC substrate which requires cumbersome preparation and is also complicated to transfer of graphene sheets from SiC²¹.

In CVD, a gaseous carbon source usually consisting of methane and hydrogen gas is heated to high temperatures ($800\text{-}1500^\circ\text{C}$) to break C-H bonds in order to form graphene on the substrate surface. Catalytic metals are often used to reduce heat-temperature requirement²². By using CVD, graphene can in principle be grown on any substrates including non-catalytic substrates. In practice, growth is mostly done on a transition metal support²³, where especially frequently used are Cu²⁴⁻²⁶ and Ni^{27,28}. As shown in Fig. 1.2, Cu has good catalysis for graphene growth, and low solubility of carbon in Cu can limit the graphene growth to a surface process²⁹. Ni has a low lattice mismatch³⁰ and a strong interaction by weak adsorption due to hybridisation between C π -orbital and Ni d_{z^2} .³¹

**FIGURE 1.2**

Growth mechanism of CVD-produced graphene on catalytic Ni or Cu. (Reproduced with rights from ref.²² copyright 2013 Wiley-VCH Verlag GmbH & Co. KGaA, Weinheim)

CVD or epitaxial growth can produce very large single graphene sheets, among which most notably is the report of a 30-inch roll-to-roll graphene film by Lijima *et al.*³² (Figure 1.3). In this case, CVD was used to grow graphene monolayer sheets on flexible Cu foil substrate, and these sheets could be stacked layer by layer to form four-layer film with 90% transparency and a surface resistance of $30 \Omega \text{ sq}^{-1}$.

**FIGURE 1.3**

Schematic illustration of roll-based graphene grown on Cu foil reported by Lijima *et al.* (reproduced with right from ref.³² copyright 2010 Macmillan Publishers Limited.)

The mostly concerned setback of growing graphene is the presence of grain boundaries resulting in polycrystalline graphene sheets^{33,34}, due to nucleation starting from multiple sites on the substrate. Grain boundaries reduce the outstanding properties of graphene^{35,36}. Another drawback is the high amount of energy required for growth conditions, making it be a very high-cost way to produce in industrial scale²³. Finally, transfer from support substrates is often challenging and potentially damaging to graphene sheets, and thus new methods for transfer is being developed^{37,38}.

Top-down exfoliation of graphite to graphene

Solvent exfoliation is another method to produce graphene on a large scale. The main challenge is to completely separate individual layers. This can be achieved by stabilization effects at solid/liquid interfaces to facilitate separation and to prevent from aggregation, where interfacial tension plays

a key role in dispersion of a solid in liquid³⁹, as the inter-layer interactions, π - π stacking and van Der Waal's forces, are weak 7 kJ mol^{-1} of carbon⁴⁰.

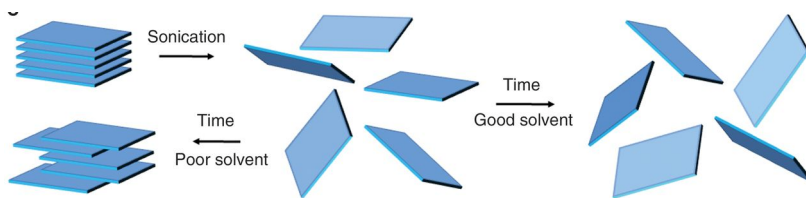


FIGURE 1.4
Schematic illustration of basic principles in liquid exfoliation

The energy required to break the weak interaction between the graphene sheets is most often provided by vigorous sonication for extended time. To minimize the interfacial tension for a stabilized graphene exfoliation, the surface energy of graphene and solvent should be as close as possible. Graphene surface energy is predicted to be similar to nanotube and graphite (70 mJ m^{-2})⁴¹ which correlates to a surface tension $\gamma \approx 40 \text{ mJ m}^{-2}$,⁴¹ making N-methyl-2-pyrrolidone (NMP) $\gamma = 40.25 \text{ mJ m}^{-2}$,⁴² N,N-dimethylformamide (DMF) $\gamma = 39.07 \text{ mJ m}^{-2}$,⁴³ and dimethyl sulfoxide (DMSO) $\gamma = 41.76 \text{ mJ m}^{-2}$; some of the best solvents for exfoliation.⁴³ Indeed, successful solvent exfoliation has been reported in NMP $\approx 1 \text{ mg mL}^{-1}$ with long sonication time $\approx 500\text{h}$, about 25% of the sheets are mono-layer and the majority <5 layers⁴⁴, this exfoliated graphene can be up-concentrated to a 20 mg mL^{-1} stable dispersion⁴⁵. There are, however, possible problems with the use of these solvents. They are toxic^{46,47} and have high boiling points, which can make it problematic to completely remove solvent residues. Therefore, several attempts have been reported using less toxic and lower boiling point solvents. Water would be the best choice from a green point of view. However, water's poor interaction ($\gamma = 71.99 \text{ mJ m}^{-2}$)⁴⁸ with the hydrophobic surface of graphene makes it impossible to directly exfoliate graphite into graphene in pure water. Some limited success has been reported using ethanol, acetone and acetonitrile⁴⁹.

In order to make exfoliation in water possible, the use of surfactants has been extensively studied⁴⁹. For example, particularly interesting are intercalating surfactants such as pyrene salts have been used by Green and co-workers⁵⁰ to stabilize dispersion of graphene in water of $0.8\text{--}1.0 \text{ mg mL}^{-1}$. A number of polymers have also been used to stabilize graphene in aqueous dispersion⁴⁹. They do help stabilization of graphene nanosheets, but do not reach the same extent as pyrene salts do.

The main benefit of solvent exfoliation over CVD is the fact that the produced graphene sheet does not contain crystal defects, as they are broken down from large crystalline graphite. Also, this method is easier to effectively scale up. The down side is that the sheet size is normally small^{51,52} $\approx 1 \mu\text{m}^2$ and polydispersity in thinness generating both mono-layer and multi-layered "graphene". The polydispersity problem could be solved by employing density gradient ultra-centrifugation (DGU) to efficiently separate single-layer, double-layer, and multi-layered graphene⁵³. The final challenge with this method is to get rid of the solvent and other compounds to obtain clean and pure samples, as these impurities and solvent residues all reduce the electrical properties of the product.

Graphene oxide & reduced graphene oxide

Finally, wet-chemical exfoliation can be done by chemical oxidation of graphite into graphite oxide

(GO) (Fig. 1.5), which is in turn exfoliated to single layers in water. GO can then be reduced to reduced graphene oxide (RGO). This method is by far the easiest way to scale up and arguably the most efficient approach for large scale production. However, the reduction of GO back to graphene is not a complete restoration, resulting in significant structural defects remained in RGO.

Graphite oxide is by no means a new material, but the knowledge that it is a truly two-dimensional material was missing. Brodie first synthesized graphite oxide, i.e. the un-exfoliated graphene oxide in 1859⁵⁴. Brodie investigated the fundamental properties of graphite oxide. He oxidized graphite using KClO_3 in fuming nitric acid over four reactions, and he found that the maximal oxidation he could achieve, is graphite oxide with a C:O ratio of $\approx 2:1$. Brodie observed that graphite oxide was soluble in water, but what he did not realize was that at this point he was probably the first person ever to prepare a two-dimensional material of atomic height suspended in water, because it was at that time impossible to directly measure the thickness of such a material. Staudenmaier improved the method of preparing graphite oxide in 1898⁵⁵ by adding sulfuric acid to the reaction mixture and KClO_3 in several fractions, thereby obtaining the fully oxidized graphite oxide (C:O $\approx 2:1$) in a single reaction. Today, the most commonly used way of producing graphite oxide is the Hummer's method with various modifications, which was developed in 1958 by Hummers and Offeman⁵⁶. They substituted the oxidant to KMnO_4 and used only sulfuric acid as solvent and acid. This method can achieve a similar level of oxidation.

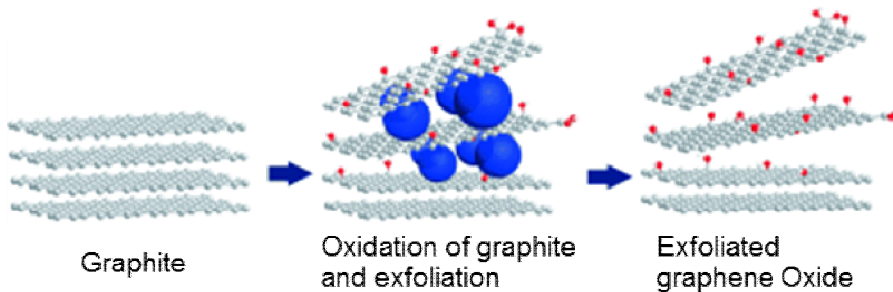


FIGURE 1.5

Schematic representation of oxidation and exfoliation of graphite into graphene oxide (adapted with right from ref.¹⁹ copyright Wiley-VCH verlag GmbH & Co. KGaA, Weinheim)

Graphite oxide prepared by either of these methods or variation thereof, undergoes significant structural changes. The conjugated sp^2 carbon network is partially changed into a sp^3 network decorated with oxygen groups, removing all electronic properties of graphene transforming it into an insulator. The electronic properties can be restored partially by reduction in the form of RGO⁵⁷. The material has new interesting properties such as easy exfoliation into a 2D material and high chemical reactivity making surface functionalization feasible. The graphite oxide can be exfoliated in slightly acidic, neutral or alkaline aqueous solution at high concentration. Water intercalates^{58,59} and separates the sheets in solution, so that graphene oxide will have a net negative charge resulting in electrostatic repulsion helping the exfoliation into single-layer graphene oxide sheets⁶⁰. Practically the exfoliation is helped significantly by either sonication or intensive stirring. Sonication results in fractured graphene oxide sheets, just as graphene sheet reducing the average size of the sheet^{51,52}. Other polar solvents can also be used for the exfoliation of graphene oxide, i.e. ethylene glycol, DMF, NMP and THF⁶¹. After exfoliation, high-speed centrifugation can be used to separate exfoliated graphene oxide from stacked graphite oxide. One of the issues that make GO difficult to study in detail is the fact that the product of graphite oxidation exhibits a batch-to-batch variation,

arising from a number of reaction conditions, i.e. heat, oxidant acid, source of graphite and so forth⁶². Dimiev *et. al.*⁶³ discovered that the work-up after oxidation, also has very big impact on the produced graphene oxide. They performed experiments where they skipped aqueous work-up after preparing graphite oxide based on the Hummer's method. Instead, they used different organic solvents for the work-up and removal of H₂SO₄ and KMnO₄. The results showed that the prepared product was not a grey graphite oxide but yellow and in some cases white. They explain this by the hypothesis that after oxidation most of the sp³ hybridized basal plane is covered with epoxides or covalent sulfur species. During aqueous work-up some of these are hydrolyzed, and partial sp² hybridization is restored resulting in an increased absorption of light.

The structure of GO is an exceeding complex, and therefore the chemical structure has been a study of much debate in scientific community. The complexity of graphene oxide stems from several factors, and it is a non-stoichiometric amorphous material with sample-to-sample variations difficult to be characterized precisely. Over the years, several models have been proposed. The first model proposed by Hofmann⁶⁴, Scholz-Boehm⁶⁵ and Nakajima-Matsuo⁶⁶ has regular lattices and compositions. It is now generally believed that the structure of GO is truly amorphous. The most known and cited model of graphene oxide was proposed by Lerf and Klinowski⁶⁷ and is based on solid state NMR measurements of graphite oxide (Fig. 1.6).

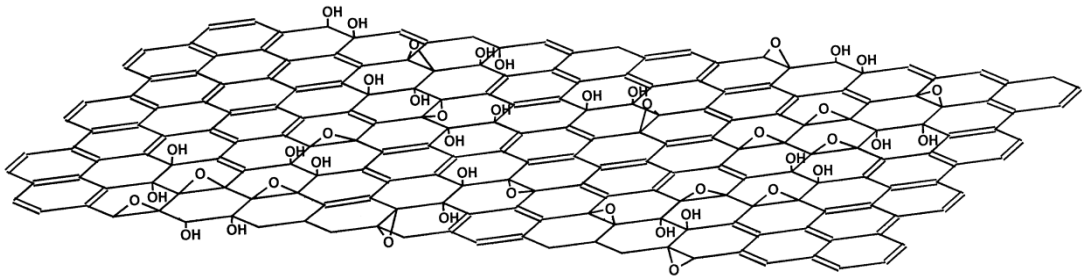


FIGURE 1.6
Structural model of graphite oxide proposed by Lerf and Klinowski⁶⁸

The NMR measurements confirm what the previous models already predicted in terms of functional groups, based on chemical reactivity. Namely, tertiary alcohols ($\delta = 60$ ppm), epoxies ($\delta = 70$ ppm) and alkenes or aromatic ($\delta = 130$ ppm). The results still cannot fully elucidate the distribution of these groups or whether the alkenes are separated or clustered in conjugated or aromatic assemblies⁶⁹. With further synthetic experiments, Lerf *et. al.*⁶⁷ finally concluded that these double bonds were likely either aromatic or part of conjugated systems because isolated double bonds are unlikely to resist the strongly oxidative media.

The fact that oxidation of graphite makes exfoliation simple but also removes the most significant properties of graphene namely electronics, has made research into reducing graphene oxide back into graphene an area of particular interest. Reduction of graphene oxide can be achieved by a long list of different methods⁷⁰. However, the resulting product is not pristine graphene, because it so far has not been possible to completely restore the structure of graphene and the properties that follow with it. Although the properties are not matching those of pristine graphene, RGO is highly interesting for many of the applications that have been proposed for graphene due to its cheap large-scale production and similar properties⁷⁰.

One of the first and still the most common method of chemical reduction of graphene oxide was introduced by Ruoff and co-workers⁷¹, where hydrazine monohydrate was used as the reducing

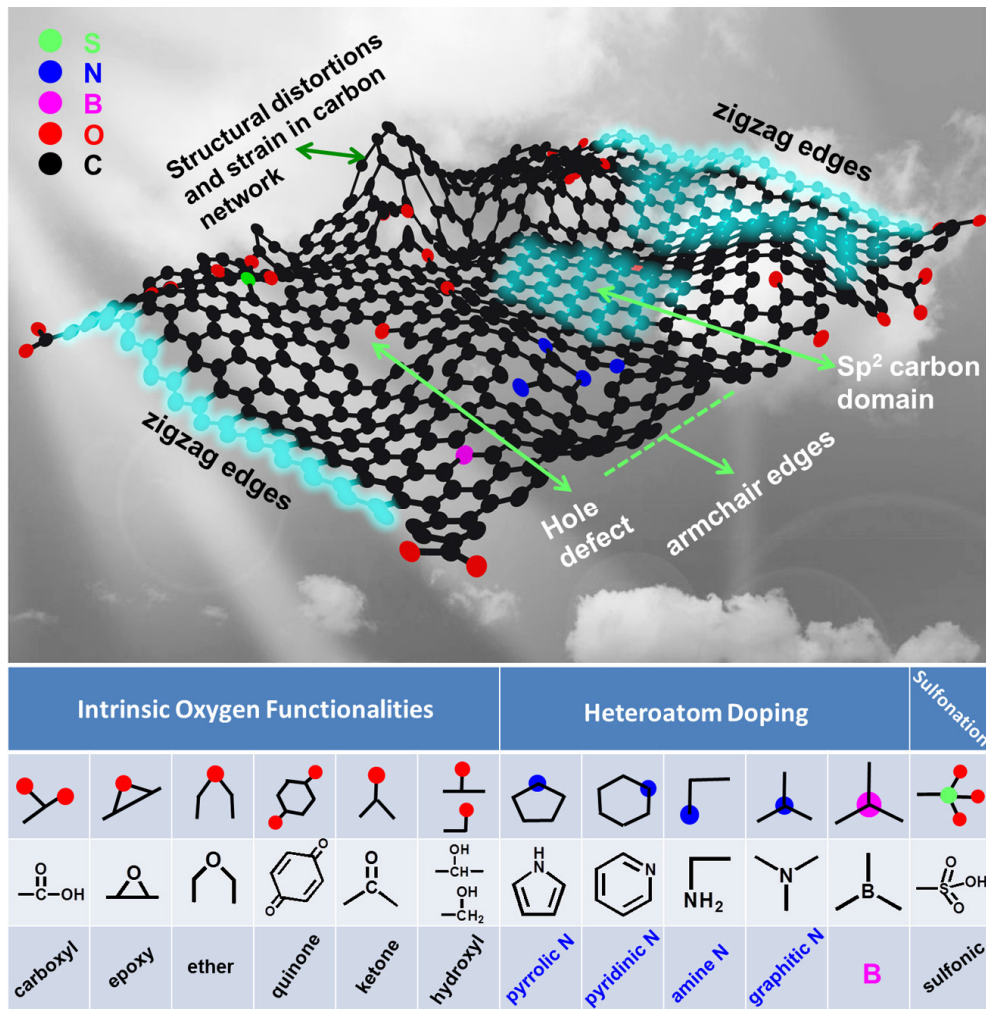
agent. The main reason for using hydrazine as compared to other strong reducing agents is its stability in water. Hydrazine effectively reduces GO into RGO, removing many of the oxygenated functional groups on the graphene sheet, and restoring the conjugated sp^2 network largely. However, some structural defects and functional groups remain. RGO is not a well-defined product and sample-to-sample variation is even more pronounced. Hydrazine reduced RGO has an oxygen content around C:O = 10:1.⁷¹ The main carbon species left as determined by either NMR or XPS is C=C, some COO- groups retaining at the edges. The conductivity can be restored to a degree of 780 $k\Omega\ sq^{-1}$.⁷² One disadvantage of hydrazine is introduction of nitrogen functionalities because hydrazine is also a nucleophile introduction of amine functionalities is commonly see these impurities can amount to C:N = 16:1.⁷¹

A more efficient method to reduce graphene oxide is by using sodium borohydride ($NaBH_4$). Despite the fact that $NaBH_4$ is unstable in aqueous solution, it can be used for aqueous reduction of GO because the decomposition is kinetically slow. After reduction with $NaBH_4$ the sheet resistance is reduced to 59 $k\Omega\ sq^{-1}$ significantly lower than for hydrazine⁷². Other chemical methods have been reported using a variety of reducing agents^{73,74} including green methods using mild reducing agents such as ascorbic acid^{75,76} to reduce GO to some extent. However, they are not as efficient as hydrazine or $NaBH_4$. Many methods utilize in situ generated H_2 using metals in acid^{77,78}. Interestingly, it has also been reported that GO can be reduced in strong alkaline solution without the use of reducing agent⁷⁹. Thermal reduction⁸⁰ at high temperatures about 1000 °C is another highly used method of reducing GO sometimes in combination with H_2 atmosphere. This work by releasing oxygen in the form of CO or CO_2 effectively leaving behind structural defects⁸¹. Despite these defects the bulk conductivity amount to 1000-2300 $S\ m^{-1}$.⁸² Finally, GO can be reduced electrochemically^{83,84} highly effective able to reduce the oxygen content to C:O = 24:1 and generating films with conductivity of 8500 $S\ m^{-1}$. However, this method could suffer from problems to efficiently scale up⁶².

Functionalization of graphene materials

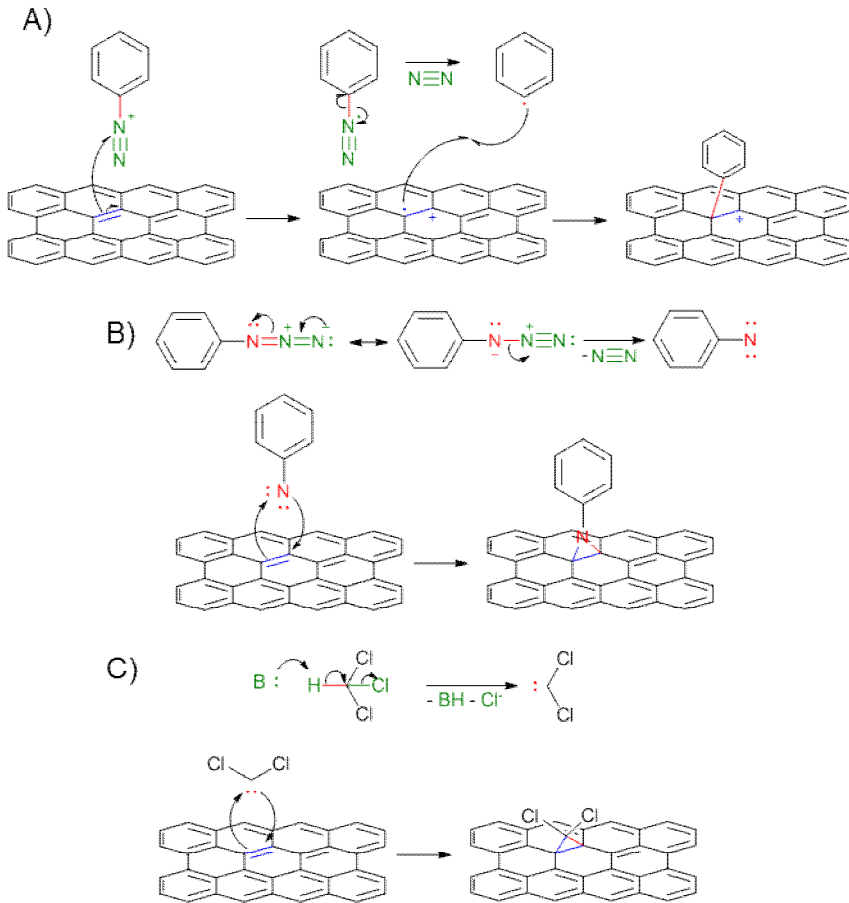
Chemical functionalization of graphene is an area of high interest. The possibility to fine-tune properties, introduce a band gap or generate selective binding to graphene has a wide range of potential applications⁸⁵. This is done either by doping⁸⁶ i.e. incorporation of heteroatoms into the graphene network, by non-covalent attachment⁸⁷ or by covalent functionalization of edges or basal plane; here we focus on covalent functionalization of graphene, RGO and GO.

Pristine graphene is generally chemically inert and therefore difficult to functionalize due to high bond energy in the structure⁸⁹. However, functionalization is feasible at the edges of graphene, due to carbons with unpaired electrons and edge defects, increasing the reactivity of the otherwise inert graphene⁹⁰⁻⁹². Edge functionalization can be used to improve solubility and change assembly behavior⁹³. However, edge modification only changes a fraction of the graphene surface area and provides limited functionalization. Introducing only edge functionalization the sp^2 network remains intact; therefore, edge functionalization does not radically change electronic properties such as electron mobility and band gap.⁹⁰

**FIGURE 1.7**

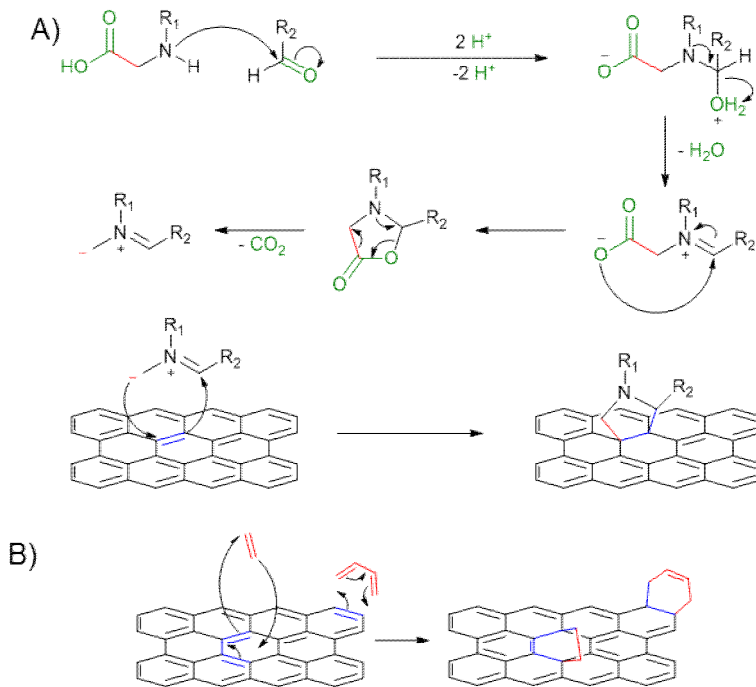
General schematic model illustrating possible active site for functionalization in graphene, oxidized graphene and doped graphene. Reproduced from ref⁸⁸ with permission copyright 2014 Elsevier B.V.

Chemical functionalization of basal plane in pristine graphene is challenging, because functionalization of a carbon changes it from sp^2 to sp^3 . Thereby, the geometry change which is energetically unfavorable and therefore requires highly reactive intermediates⁸⁹. Furthermore, change from sp^2 to sp^3 carbon will result in a disruption of the π -conjugation. Functionalization is therefore a trade-off of introducing new properties at the expense of some of the existing electronic properties. Functionalization of the basal plane can be achieved by free-radical reaction, usually using diazonium salts to generate carbon radicals, which can react with the chemically inert graphene^{94,95}. The main disadvantage of using free radical reaction for graphene functionalization is possible side reactions that could occur simultaneously, which can in some cases limit the use.

**FIGURE 1.8**

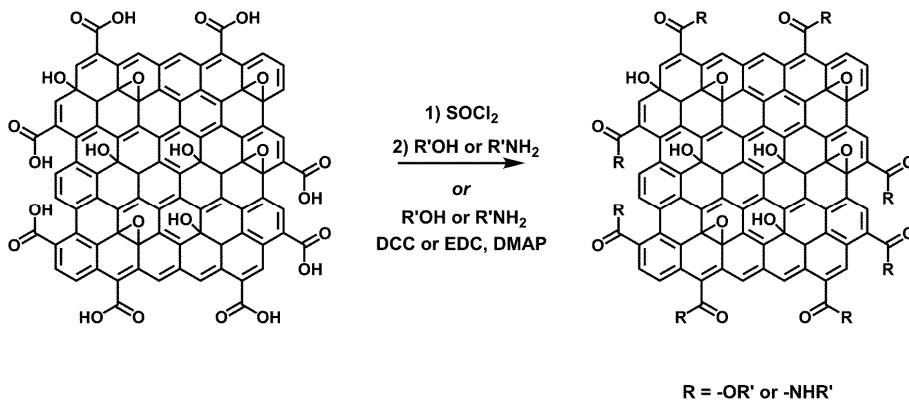
Schematic mechanisms of the possible reactions: A) radical addition to graphene initiated by diazonium salt by production of free nitrogen, B) *in situ* formation of nitrene from azide, which is added to graphene in a [1+2] cycloaddition; and C) base induced formation of carbene also reacting in a [1+2] cycloaddition with graphene

In the functionalization of related carbon materials C_{60} and nanotubes, cycloaddition reaction has shown to be a powerful tool and indeed these reactions are also useful in functionalization of graphene: [1+2] cycloaddition of a carbene^{96,97} or nitrene^{98,99} with two graphene carbons to form a 3-membered ring can be used due to the high reactivity (Fig. 1.8). As shown in Fig. 1.9, another possibility is the use of [1+3] dipolar cycloaddition by *in situ* generation of ylides forming a more stable 5-membered ring perpendicular to the basal plane^{100–102}. Finally, a Diels-Alder cycloaddition can be used to form 6-membered ring where graphene can function as either the diene or the dienophile^{103,104}. Despite multiple reaction are available for functionalization of graphene all of these require highly reactive intermediates, which can become problematic if the desired function groups are also reactive.

**FIGURE 1.9**

Schematic mechanism of the described reaction A) in situ formation of ylide by reaction of aldehyde and N-substituted glycine under elimination of H_2O and CO_2 . The ylide can react in a [3+2] cycloaddition with graphene. B) Diels Alder reaction between graphene and either a diene or a dienophile

Contrary to pristine graphene, the functionalization of graphene oxide is surprisingly approachable. Many functional groups in GO introduce the possibility of reactions with both nucleophiles which can react with epoxides and activated carboxylic acids, and electrophiles reacting with hydroxyls and carboxylic acids. The main challenge is to selectively control the functionalization, as there are several different types of functional groups in GO that can be used to functionalize it.

**FIGURE 1.10**

Schematic illustration of edge functionalization carboxylic acid by activation followed by coupling with amine. (Reproduced from ref¹⁰⁵ with permission copyright The Royal Society of Chemistry.)

Edges of GO is decorated with carboxylic acids which can be activated by a wide variety of reagents such as SOCl_2 ¹⁰⁶, EDC¹⁰⁷, DCC¹⁰⁸ and then functionalized by nucleophiles coupling moieties onto the graphene oxide edges (Fig. 1.10). The most common method use for functionalizing the edges of GO is by using EDC coupling with amines forming stable amides, the only concern here would be “accidental” functionalization of basal as well given nucleophilic ring opening of epoxides. Basal plane functionalization of GO is possible by nucleophilic ring opening of epoxides where a nucleophile attacks the α -carbon of the epoxide opening the epoxide into a hydroxyl at the β -carbon^{109,110}. Graphene oxide can also be functionalized by electrophilic isocyanates that can react with edge carboxylic acids to create carbamate esters or with hydroxyl groups on the basal plane forming amides¹¹¹. The more aggressive functionalization methods used for pristine graphene are also possible for graphene oxide but rarely used, because there are milder functionalization methods available.

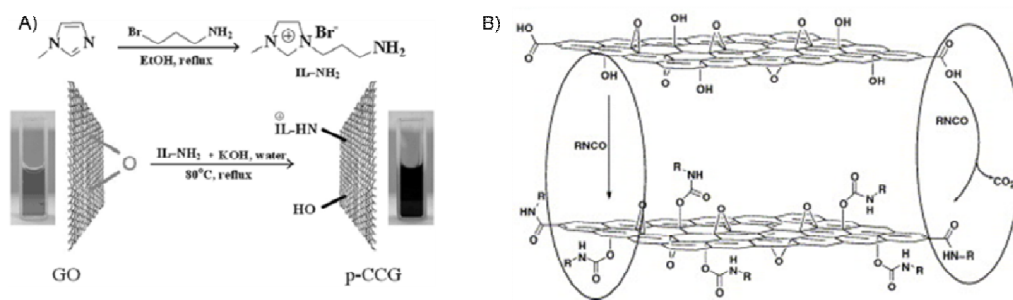


FIGURE 1.11

Illustration of basal plane functionalization A) by nucleophilic ring opening of epoxides and B) using isocyanate functionalization. (Reproduced from A) ref.¹¹² with permission copyright The Royal Society of Chemistry 2009. And B) ref.¹¹¹ with permission copyright Elsevier Ltd. 2006)

Compared to GO, the chemical reactivity of RGO is significantly reduced. Therefore, chemically modified graphene prepared from RGO is usually modified before reduction. However, it is possible to modify RGO post reduction instead, this usually involves the same chemistry as those used for pristine graphene: Free radical chemistry through diazonium salt¹¹³; carbene chemistry¹¹⁴; it has been reported that residual epoxide can be utilized for nucleophilic ring opening of epoxides¹¹⁵, however, their concentration on the basal lane is reduced significantly. RGO usually retains most of edge carboxylic groups, and therefore the edge functionalization can be performed using the similar routes to those for GO functionalization.

Structural characterization

Just as GO has no unambiguous structure, it is not possible currently to fully characterize a sample of chemically modified graphene (CMG). However, a few important features are necessary to be characterized in order to evaluate CMG materials. These include topological investigation of graphene materials, the thickness of sheets to determine if they are mono-layered or multi-layered, which can be done using a range of different structural techniques: Raman, BET, AFM, TEM. Structural investigation of chemical composition to verify chemical modifications can be studied using a combination of techniques such as Raman, IR, NMR, XPS, elemental analysis, and to some degree TGA, XRD, UV-vis spectroscopy.^{116,117}

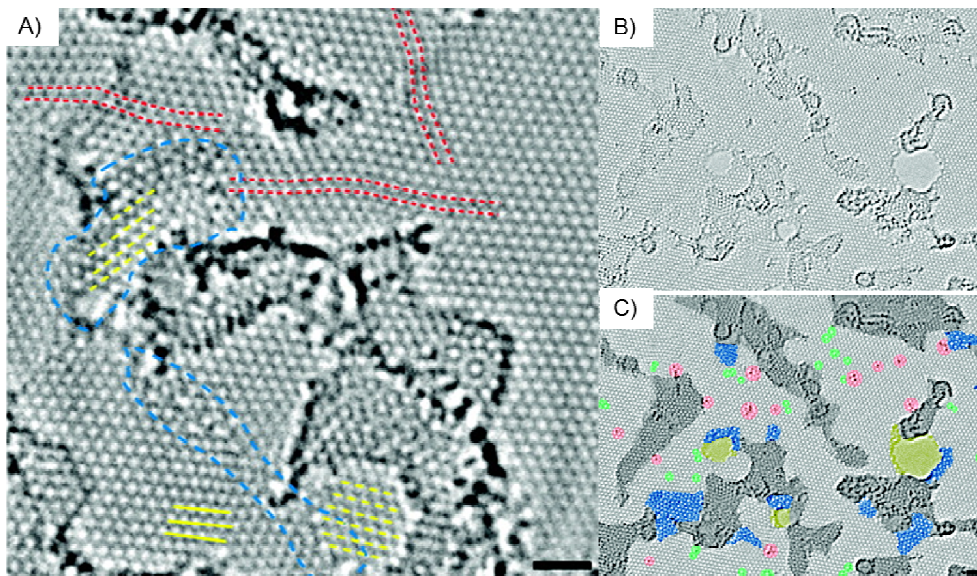


FIGURE 1.12

High-resolution TEM images of A) chemically derived graphene monolayers identifying the specific atomic scale features that originate from the oxidation–reduction treatment of graphene. B) & C) Atomic resolution, aberration-corrected TEM image of a single layer reduced-graphene oxide membrane. (B) Original image and (C) with colour added to highlight the different features. (Reproduced from A) ref.¹¹⁸ with permission copyright American Chemical Society 2010)

Microscopic imaging techniques are essential for elucidating structural features of nano-materials including graphene and chemically modified graphene. AFM¹¹⁹ and TEM¹¹⁸ can provide detailed information of shape, size and thickness at the appropriate resolution to study graphene materials and even structural defects within them. Raman can be used indirectly to evaluate the thickness of graphene sheets by assessing the ratio between D band (associated with disorder) and G band (associated with the stacking). A high D/G ratio indicates high exfoliation¹²⁰. Finally, the specific surface areas can be measured by the BET method and compare them with the theoretical surface area of graphene.

Information about the chemical composition is of paramount importance in chemically modified graphene to evaluate if functionalization is achieved and to what extent. Elemental analysis is a strong tool for this purpose to determine change in hetero atom content. XPS is especially widely used, even though XPS is a surface technique. Due to the flatness of graphene, XPS provides valuable information. Not only can the chemical composition be revealed to determine the presence of introduced functionalities, but also the chemical states of especially carbon atoms can offer essential information. The carbon 1s peak can be de-convoluted into the characteristic peaks at 284.4 eV (C-C sp²), 285.2 eV (C-C sp³), 286.4 eV (C-O), 287.7 eV (C=O) and 289.1 eV (COO)¹¹⁶, respectively. The deconvolution gives direct information of the reduction extent not only in terms of reduced oxygen content but also reformed sp² hybridization. Also, the nitrogen 1s peak can be deconvoluted to give additional information of the chemical state which in many cases is important to evaluate functionalization.

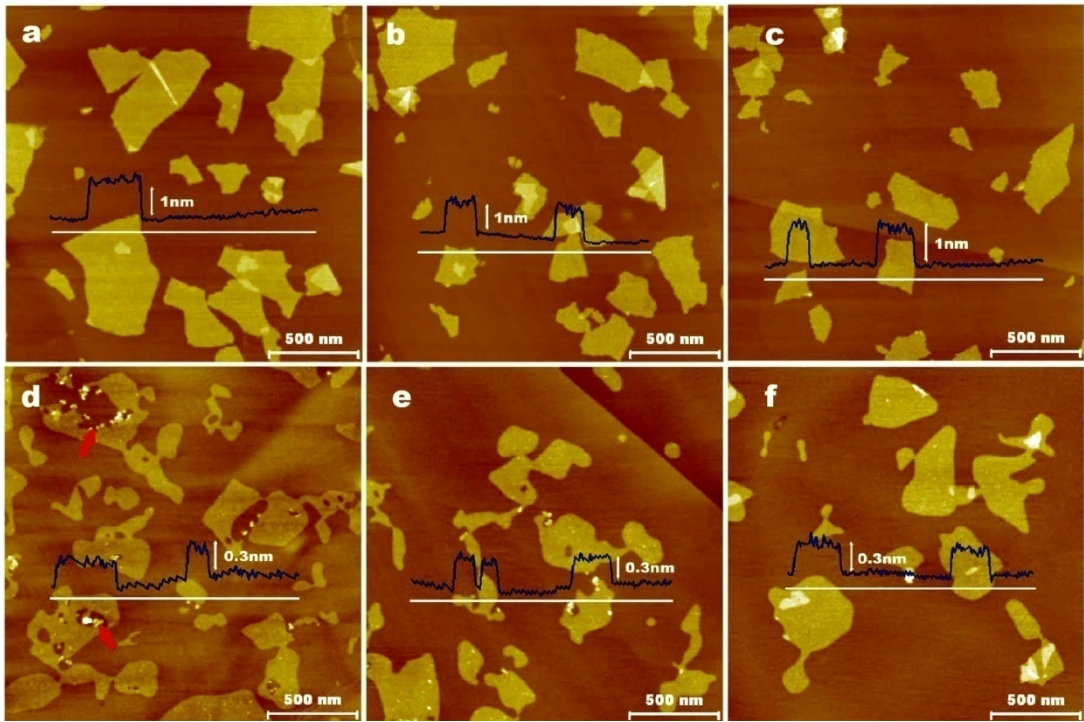
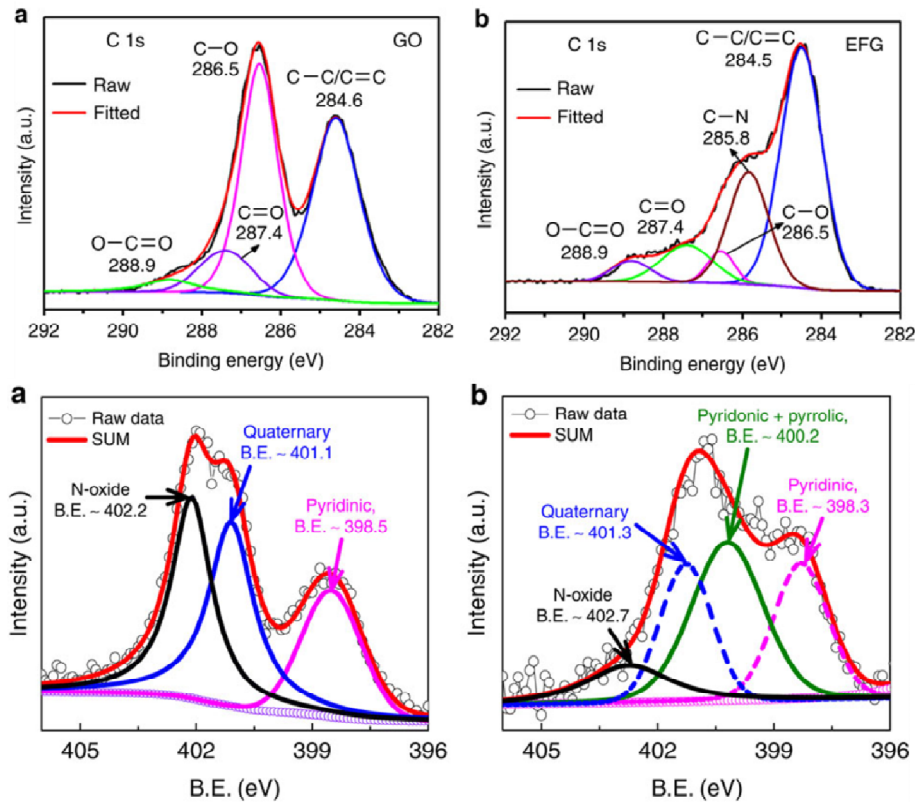


FIGURE 1.13

Nanometer-scale AFM images for the unreduced (a,d), mildly reduced (b,e) and highly reduced (c,f) graphene oxide sheets deposited on top of an HOPG substrate, prior to the thermal treatment (a–c) and annealed at 1773 K (d–f). (Reproduced from ref.¹²¹ with permission copyright The Royal Society of Chemistry 2015)

In the structural determination of small compounds, liquid phase ^1H and ^{13}C NMR play an important role. However, because of the large size of graphene sheets rotation in liquid phase is slow resulting in anisotropic coupling in NMR which is the reason liquid phase NMR is not used for structural information of chemically modified graphene. Solid phase magic angle ^{13}C -NMR is however used and as for XPS give valuable information of the chemical state of the carbon in graphene.^{58,59,67,69,116}

Vibrational spectroscopy is an important tool using either IR or Raman spectroscopy to determine functional groups in graphene, based on their fundamental vibrations.^{116,117}

**FIGURE 1.14**

XPS characterization of carbon materials A & B) C 1s XPS spectra of **A)** GO, **(b)** functionalized RGO (**)** C and D) Deconvoluted N1s spectra for carbon nanofibers A) before and B) after electrochemical treatment (A & B Reproduced from ref.¹²² and C and D from ref.¹²³ with permission copyright Macmillan Publishers Limited. 2014 and 2013)

Graphene functionalized with supramolecular moieties for Sensing

Chemicals in general from Essential to toxic compounds and even simple Ions have a tremendous impact on our body functions, health and diseases. Therefore, detection or monitoring of specific compounds or ions in our body could be crucial for diagnostics^{124,125}. The increase in environmental awareness also implies a growing need for sensitive detection of chemicals from the water supplies to the air quality^{126,127}. Chemical sensors for explosive¹²⁸ and chemical warfare agents¹²⁹ are also increasingly important in demining previous warzone, air security, and other security in risky areas. In general, a sensor is a device that can detect and convert an input stimulus into a readable output, i.e. a motion sensor can detect motion and covert this stimulus into signal like an alarm or electrical recording. A chemical sensor is a sensor, which can recognize a specific chemical and give an output allowing us to identify that specific compound in a mixture of many compounds. Thus, chemical sensor has two main functions. One is selectivity, which has to be able to selectively recognize specific compound out of a mixture. The other is transduction, which enables the conversion of specific stimulus of one compound into a readable signal. The signal could be

optically sensing such as colorimetric¹³⁰, fluorescent¹³¹ and circular dichroism based¹³²; or electrochemically sensing such as potentiometric¹³³, amperometric¹³⁴, conductometric¹²⁷; thermometric¹³⁵ etc.

Due to this dual functions required, one rational design of sensors is to have a recognition unit or binding site covalently link to a probe also called the “receptor-spacer-reporter approach”¹³⁶, which is indeed a recurring design for synthetic molecular sensor¹³⁷.

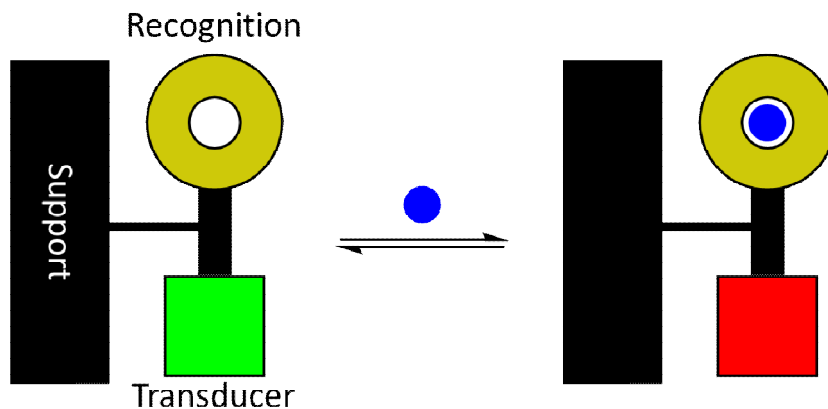


FIGURE 1.15

Schematic of supported “receptor-spacer-reporter” type sensor

Selectivity is a major concern for sensors. There are two main ways to tackle the problem of selectivity in a chemical sensor. One is direct sensing and has its origin in “the lock and key principle” first postulated by Emil Fischer in 1894, in which a recognition unit has a very high affinity towards one specific compound thereby generating a one-to-one relationship between stimuli and sensor output. Examples of this approach include biological signaling receptors such as seven-transmembrane receptors¹³⁸, antibody recognition system¹³⁹, synthetic sensors¹³⁶ or molecular imprinting¹⁴⁰.

The benefit of this approach is one-to-one identification of a compound, resulting in a very high selectivity for sensors with perfectly matched to the compound. The drawback is that some compounds are extremely similar structurally, and thus a perfect sensor is hard to construct if not impossible. Even in biology, many systems that have evolved over millions of years can be still basis of medicinal chemistry to find alternative molecules to trigger certain receptors. Another potential drawback is the need for one unique sensor for each compound.

The other approach is array has its origin in olfactory sensing where a series of sensors are connected each sensing different properties of a compound and the collective signal is then analyzed in order to identify the specific compound. The benefit of array sensing is that the use of many sensors, enable the detection of an even larger library of compounds, by using data from each receptor to piece together the compounds. One drawback of such a system is its inherent complexity, as it needs multiple receptors that together crate a complete array. Another drawback is that in mixtures of compounds two or more compound can be interpreted as one and thereby give positive detection where it should give a negative result, this is avoided by having sufficient sensors to create unique sensing finger-print.

Graphene, RGO and CMG has been shown to be useful in the area FET sensors due to electronic properties and high surface area, for RGO and CMG also low production cost is a big advantage over similar materials^{141,142}. RGO has been used as a resistance type sensors based on FET for the

detection of gaseous NO_2 ; where adsorption of NO_2 gas due to its electron withdrawing abilities increasing the conductivity the sensor show high sensitivity capable of detecting 1.56 ppm NO_2 ; ¹⁴³ furthermore the sensor can also detect NH_3 gas where due to electron donation the resistance is increased however less sensitivity in this case shown current decrease at 1% exposure further development has been made on these type of sensors ¹⁴³. However the fundamental problem is selectivity the mechanism of detection rely on electron density so any absorbent can change the current output make interference a major problem.

RGO and CMG has shown high promise in electrochemical sensors their good conductivity and high surface area combined with electro catalytic properties instilled by residual or purposefully attached functionalities, these functional group can also provide a small selectivity towards some molecules however the real selectivity of graphene based electrochemical sensors comes from separation from redox peaks inherent in all electrochemical sensors. Still interference is a problem as similar compounds still have similar redox potential.

Ionophore functionalized graphene for ion sensing

Supramolecular host molecules ionophores has for decades been using in chemical sensing of cations and anions alike, due to multiple directive interaction these host molecules gives highly selective binding of specific ions. Ionophores such as crown ether ¹⁴⁴, and Schiff base complexes ¹⁴⁵, has been uses extensively for sensors of different types to selectively bind and detect ions ^{146–148}.

Despite the immense body of work being done with graphene based sensors and relative ease of functionalization of graphene via GO or RGO to make CMG surprisingly few reports show direct functionalization of graphene with ionophores. Ionophores are however extensively used for graphene based potentiometric sensors using ion-selective membranes with ionophores ^{149–153}.

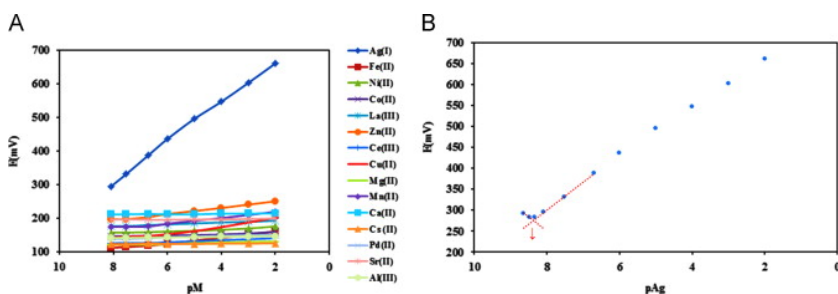


FIGURE 1.16

A) Response to various cations of potentiometric modified CPE sensor. (B) Calibration curve of the Ag(I) modified CPE sensor. (Reproduced from ref. ¹⁵⁴ with permission copyright Elsevier B.V. 2014)

Afkhami et. al. ¹⁵⁴ have shown that their graphene paste based potentiometric sensor incorporating graphene nanosheets and molecular wire as conductive binders and thione as a silver(I) ionophore mixed into a carbon paste electrode material. This electrode material can efficiently detect trace amounts of silver in aqueous solutions down to a detection limit of $4 \times 10^{-9} \text{ mol L}^{-1}$. They have also shown that this sensor is highly selective showing no interference from any of the many cations they tested (fig. 1.16), furthermore they also tested several water sources mineral water, river water industrial waste both spiked and un-spiked with very high agreement with detection by ICP-OES detection. We have recently reported RGO covalently functionalized with 1-aza-18-crown[6]ether by a short flexible linker showing highly specific binding of potassium ions. This

material of drop cast onto both glassy carbon electrodes and disposable screen-printed electrode to produce selective membrane free potentiometric sensors for potassium able to detection 10^{-5} mol L $^{-1}$ of potassium ions in the presences of high concentration 10^{-1} mol L $^{-1}$ sodium ions, with no interface form other tested ions (Ca^{2+} , NH_4^+ , Li^+ and Na^+).

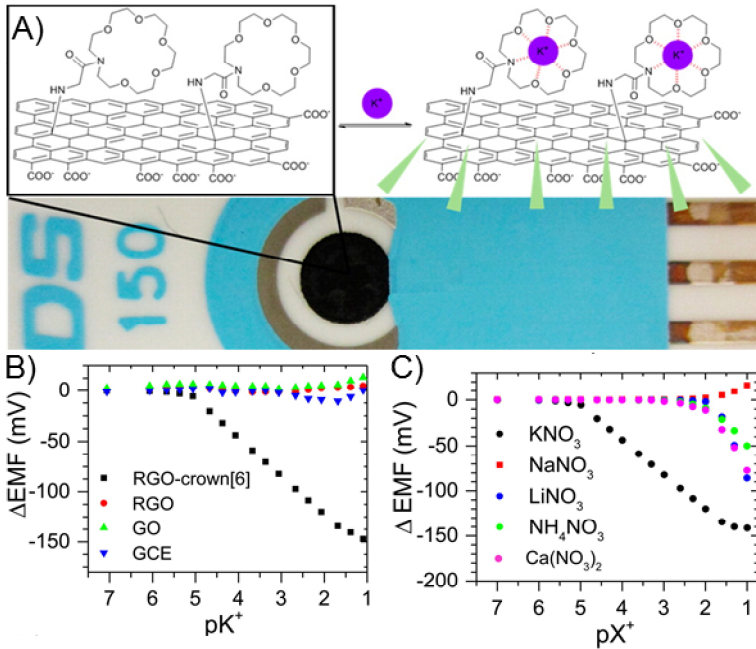


FIGURE 1.17

A) Schematic representation of sensing mechanism where selective binding of potassium ions ensure potentiometric response despite surface saturation with sodium ions B) potential response of sensing material and appropriate reference materials C) interface study with related cations. (Reproduced from ref.¹⁵⁵ with permission copyright American Chemical Society 2015)

Cavitand functionalized graphene for neutral analytes

Just as ionophores cavitands has been used for molecular recognition extensively^{156–158}. The most common cavitands are cyclodextrins, calixarenes, pillararenes and cucurbiturils. Cavitands bind their guests in binding pockets often controlled primarily by hydrophobic forces with the help of few directional bonds. Therefore their selectivity towards different size guest is very high.

Contrary to ionophores many examples of chemical modified graphene with cavitands exists especially cyclodextrines. These cyclodextrine modified CMG in have been reported as sensitive and selective sensors for a long range of biologically important analytes: Pesticides^{159,160}, medicinal compounds^{161–164} and carcinogens¹⁶⁵ by uses a combination of the size selectivity of cyclodextrines and inerrant electrochemical selectivity in form of redox potential.

Chen and co-worker¹⁶⁶ has reported the used cyclodextrine functionalized graphene in combination with differential pulse voltammetry (DPV), they show that the cyclodextrine can bind different guests in its hydrophobic cavity in this study rhodamine B and 1-aminopyrene but is easily separated in DPV this two-dimensional selectivity is the essence of how civantand functionalized

graphene electrochemical sensors work. The sensor shows high sensitivity with limit of detection for rhodamine B of 6.5 nmol L^{-1} and for 1-animopyrene 3.6 nmol L^{-1} .

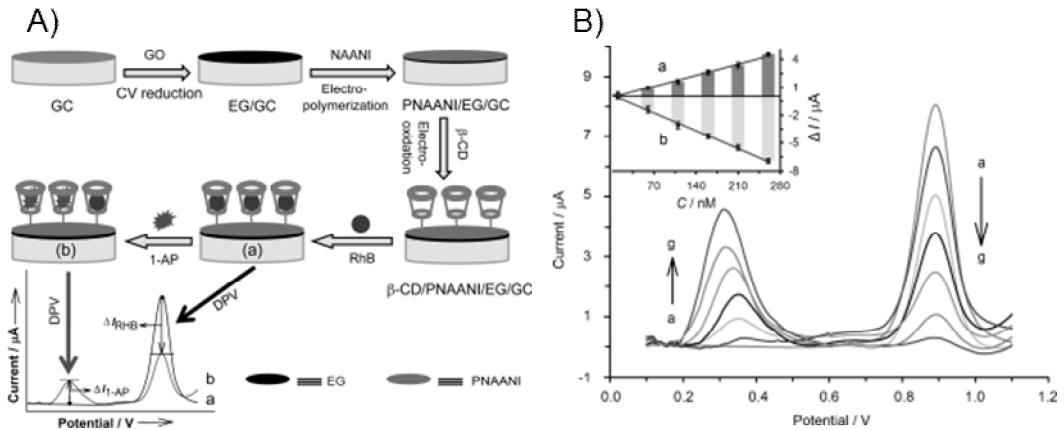


FIGURE 1.18

A) Sensing protocol of the dual-signalling electrochemical sensor based on the competitive host-guest interaction between β -CD and RhB (reporting probe)/1-AP (target). B) DPV responses at the RhB-bound β -CD/PNAANI/EG electrode in PBS (0.1 m, pH 7.0) after incubation with different concentrations of 1-AP (from a to g): 0, 10, 60, 110, 160, 210, and 260 nM; the inset shows the calibration curves for 1-AP detection based on a) $\Delta I_{1\text{-AP}}$ or b) ΔI_{RhB} as the response signal. (Reproduced from ref.¹⁶⁶ with permission copyright Wiley-VCH Verlag GmbH & Co. KGaA, Weinheim 2013)

Yang *et al.*¹⁶⁷ showed that it is possible to covalently attached the cyclodextrine to RGO and used the material in a nanohybrid with gold nanoparticles and used DVP to selectively sense p-nitrophenol and hydroquinone. Erhan Zor *et al.*¹⁶⁸ have shown the true power of this detection method by using cyclodextrine functionalized RGO to separate redox peaks on enantiomers of cystine (D-cystine and L-cystine) in DVP. They further showed that the separation is caused by different binding modes of the two enantiomers.

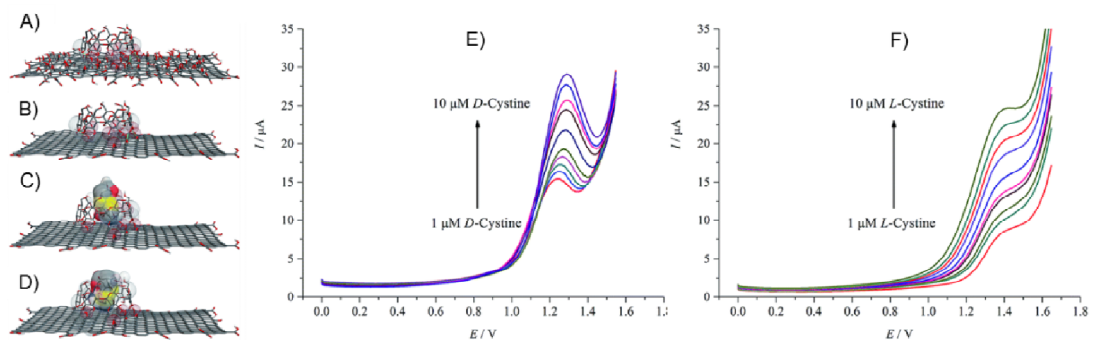


FIGURE 1.19

A-D) Computational model structures of β -CD in complexes with GO (A) and rGO (B) represented as stick models. Side view stick model of schematic drawing for the rGO/ β -CD complex with D-cystine (C) and L-cystine (D), respectively. E&F) Differential pulse voltammograms for increasing concentration of D-cystine (E) and L-cystine (F) in low concentration range (1–10 μM) at rGO/ β -CD/GCE; potential sweep rate was 0.05 V s^{-1} . (Reproduced from ref.¹⁶⁸ with permission copyright The Royal Society of Chemistry 2015)

Other cavitands are less extensively used for graphene based sensors, however calixarenes have also been used to optimized the selectivity of graphene based sensors^{169,170}. One such example is that of modified calix[4]arene imobialized on graphene by X. Mao *et. al.*¹⁷¹ which function as a highly selective chiral sensor of amino propanol by use of impedance spectroscopy with a detection limit at the nmol L^{-1} level and no interference from enantiomer.

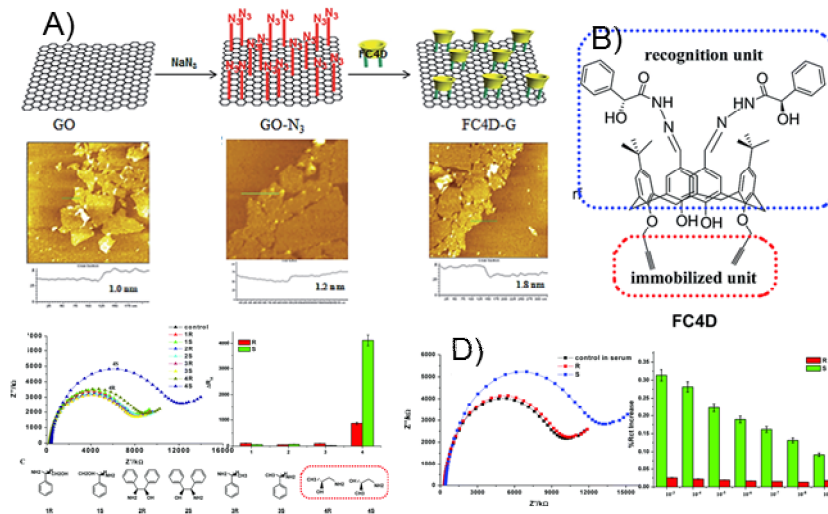


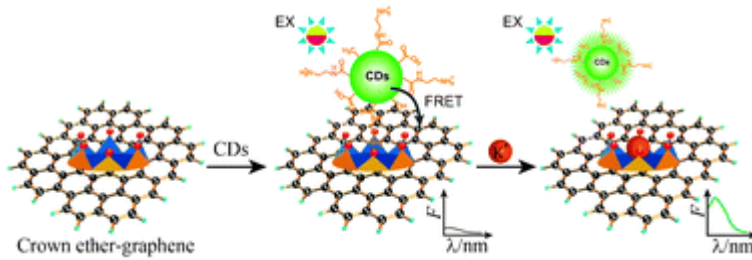
FIGURE 1.20

A) schematic of the synthesis procedure B) molecular structure of the calix[4]arene recognition unit C) Impedance response of four pairs of amino propanol analogues d) testing of sensing for the selective amino propanol analogue in serum with detection limit in the nmol L^{-1} range. (Reproduced from ref.¹⁷¹ with permission copyright The Royal Society of Chemistry 2015)

Turn-on fluorescence sensing by guest exchange of supramolecular functionalized graphene

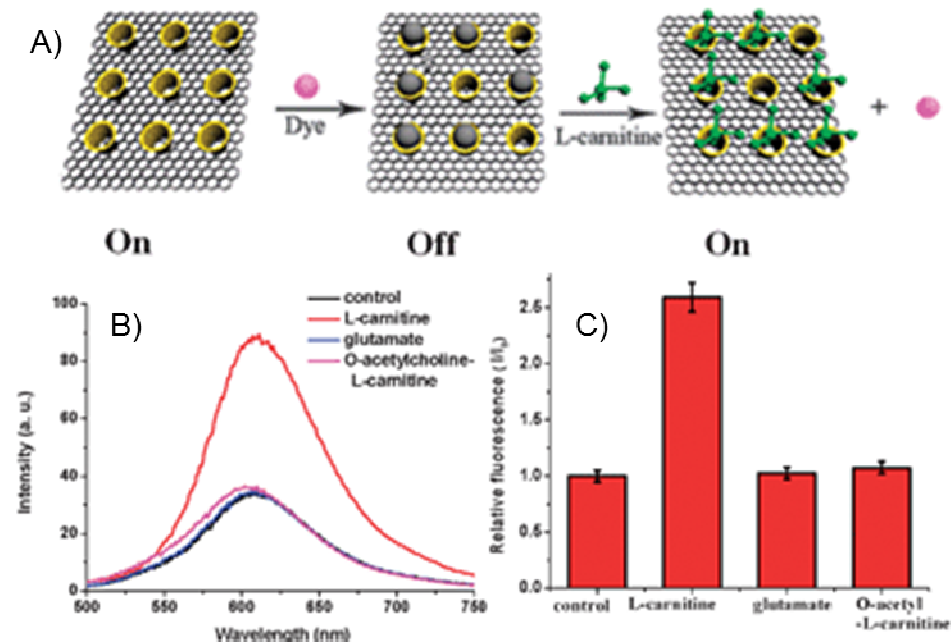
The electronic properties of graphene and by extension RGO and CMG allow for long distance ~ 30 nm quenching of fluorescence due to non-radiative energy transfer, this opens for another sensing approach^{172,173}. Turn-on fluorescence sensors can be prepared from supra-molecular functionalized graphene by coupling a fluorescence probe with a guest of the supramolecular host upon exposure to analyte competitive host-guest interaction will release the fluorophore from the graphene surface stopping the PET quenching of its fluorescence resulting in a turn-on fluorescence signal.

Qu and co-worker¹⁷⁴ used this principle to make a sensitive and selective K⁺ sensor by anchoring fluorescent carbon quantum dots on a 18-crown[6]ether adsorbed on RGO with a alkyl ammonium ion interaction with 18-crown[6]ether. Thereby the carbon quantum dots is close enough proximity to the graphene surface to quench their fluorescence. Potassium binds significantly stronger to the crown[6]ether thereby replacing the alkyl ammonium and releasing the quantum dot from the graphene surface effectively turning on their fluorescence. Their sensor gave linear response to potassium in the concentration range $5 \times 10^{-4} - 10^{-1}$ mol L⁻¹ and no interference from Na⁺ Mg²⁺ Ca²⁺ at 20 times their physiological concentration.

**FIGURE 1.21**

Schematic illustration of the FRET model based on CDs–graphene and the mechanism of K^+ determination. (Reproduced from ref.¹⁷⁴ with permission copyright The Royal Society of Chemistry 2012)

Li and co-workers¹⁷⁵ also reported a turn-on fluorescent sensor for biologically important metabolite L-carnitine in living cells. Here they immobilised p-sulfonated calix[6]arene onto RGO during the reduction with hydrazine resulting in a water dispersible CMG. They used safranin T as a fluorescent dye which due to electrostatic interaction with P-sulfonated calix[6]arene is immobilized near the graphene sheet quenching it. Detection of L-carnitine by competitive binding result in turn-on fluorescent signal with a detection limit of $1.54 \mu\text{mol L}^{-1}$. Furthermore they show that this sensor had good selectively over very similar molecules glutamate and O-acetyl-L-carnitine. Finally they showed that this sensor could be taken up into human liver cancer cell and still function as sensor *in vivo*.

**FIGURE 1.22**

A) Schematic demonstration of the fluorescence “off-on” mechanism for detecting L-carnitine. B) Fluorescence spectra of CMG–hybrid(C) Relative fluorescence intensity (I/I_0) in the presence of L-carnitine, glutamate and O-acetyl-L-carnitine, respectively. (Reproduced from ref.¹⁷⁵ with permission copyright The Royal Society of Chemistry 2012)

In a recent study, Li and co-worker¹⁷⁶ synthesized a similar p-sulfonated calix[6]arene graphene material using only NaOH at 90°C for reduction but otherwise same protocol they showed that this system also can be used to detect tadalafil a medical drug which harmful side-effects require controlled medical supervision. They use a different fluorescent probe namely rhodamine B which is quenched in a similar fashion as in Haibing Li's system. It is shown by molecular docking that Tadalafil is a good match for the sulfonated Calix[6]arene, their system give a selective detection of tadalafil with detection limit as low as $0.32 \mu\text{mol L}^{-1}$ and they show its function in human serum samples.

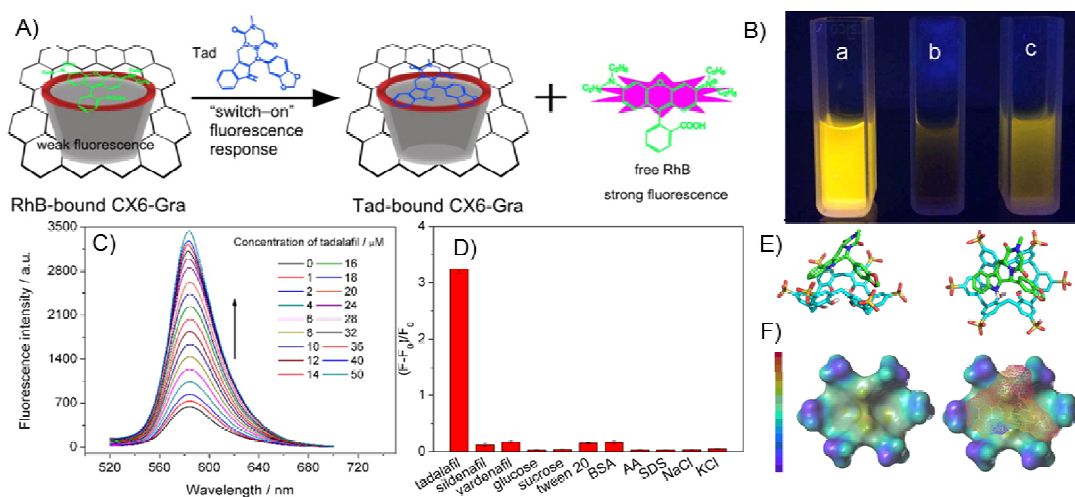
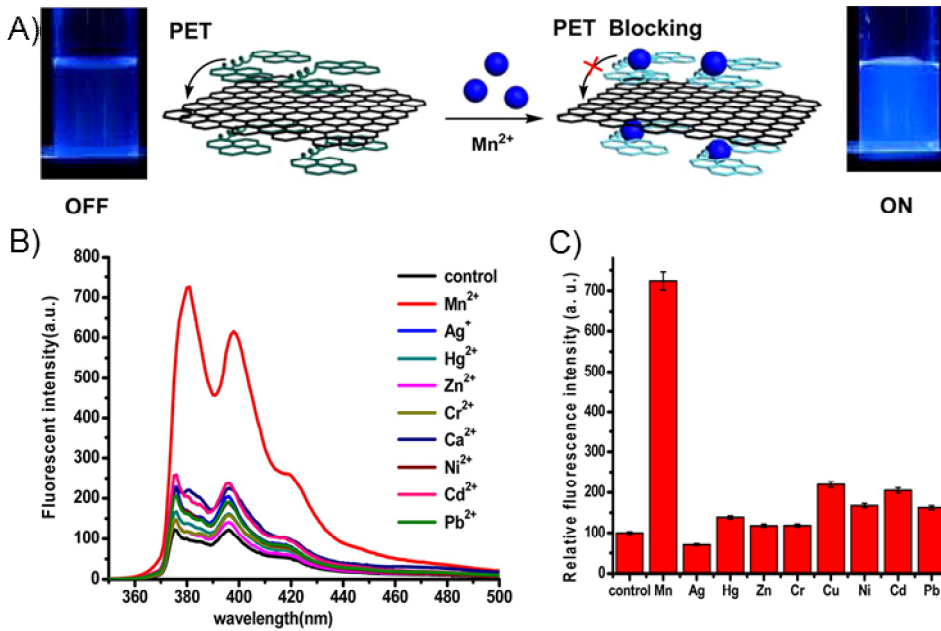


FIGURE 1.23

A) Schematic representation of Fluorescent Indicator Displacement Assay for Tadalafil. B) Photographs of a) 10 μM RhB, b) 10 μM RhB+50 $\mu\text{g mL}^{-1}$ CX6-Gra, and c) 10 μM RhB+50 $\mu\text{g mL}^{-1}$ CX6-Gra+50 μM tadalafil upon excitation under 365 nm UV light. C) Fluorescence spectra of the CX6-Gra-RhB complex vs. different concentrations of tadalafil (0–50 μM). D) Relative fluorescence intensity of interference compounds. E) Lowest energy tadalafil/CX6 docked complex (side view & top view); F) electrostatic forces distribution. (Reproduced from ref.¹⁷⁶ with permission copyright American Chemical Society 2015)

Haibing Li and co-worker¹⁷⁷ also reported the use of a graphene based turn-on fluorescence sensor in living cells this time targeting biologically important manganese(II) ions. In this study the attached supramolecular system is a 1,2-bis-(2-pyren-1-ylmethoxyamino-ethoxy) ethane (NPEY) the pyrenes binds to the graphene basal plane which quenches pyrenes fluorescence, yet in the binding to Mn^{2+} is stronger allowing NPEY to release from graphene turning on the fluorescence. This sensor has a detection limit of $4.6 \times 10^{-5} \text{ mol L}^{-1}$ and only little interference from other transition metal ions the sensor was proved to work in vivo by uptake into Hela cells in which Mn^{2+} concentration could be monitored.

**FIGURE 1.24**

A) Schematic Demonstration of Fluorescence "Turn-On" Mechanism for Mn^{2+} Detection by NPEY-GNs; with accompanying illustrative pictures. B) Fluorescence emission responses of NPEY-GNs system to different metal ions. C) The histogram directly shows the changes of fluorescence emission of NPEY-GNs at 376 nm with adding of different heavy metal ions (Reproduced from ref.¹⁷⁷ with permission copyright American Chemical Society 2013)

Biosensors based on supramolecular anchoring to graphene materials

A biosensor is an analytical device for the detection of a particular analyte, in which a biologically derived recognition entity is integrated as a transducer, to measure the quantitative change of some complex biochemical parameter¹⁷⁸. In recent years, the significance of monitoring and regulating different parameters in the areas such as clinical diagnoses, environmental protection, food industry, or forensics is rapidly increasing. Thus, there is always an urgent need for the development of reliable analytical devices with rapid and accurate analysis. Nanomaterials are showing a huge potential for the development of an efficient biosensing platform in recent years¹⁷⁹. Graphene is one of most deeply studied nanomaterials in the last decade due its extraordinary properties. Constant development with the further functionalization on graphene surface has transformed it into a unique support material for versatile biosensing applications⁸⁵.

Supramolecular chemistry is mainly focused on the interactions between molecules. Thus, the supramolecular functionalized graphene opens up a new area in the field of biosensors¹⁵⁷. Due to their unique structural properties, supramolecules can bind different kinds of inorganic, organic and biological molecules into their cavities and form stable host-guest inclusion complexes with superior selectivity¹⁵⁸. The supramolecules attached on the surface of graphene also can successfully hold the bio-recognition elements (e.g. enzymes, antibody etc.) with extra stability, which can be used a suitable biosensing platform. In addition, environmentally friendly nature of

different supramolecules and their good water dispersibility properties make them an ideal candidate for the development of different biosensing platform¹⁸⁰. Therefore, the supramolecular functionalized graphene has become a popular material for the development of wide ranges of biosensors.

Enzymatic sensors

Enzymes are the most widely used biomaterials for the development of biosensors. Due to their specific selectivity and unique catalytic properties, enzymes are popular as sensing elements in biosensing applications. A wide variety of enzymes belonging to classes of oxido-reductases, transferases, hydrolases and lyases etc.¹⁸¹ have been associated with different transducers for construction of different biosensors for applications in wide ranges of fields. The performance of an enzyme-based biosensor is dependent on several factors such as amount of enzyme loading and stability of enzyme associated with pH, temperature ionic strength etc. By tuning the immobilization method and matrix for a particular enzyme, the performance of the enzyme biosensor can be largely improved.

Different research groups had used supramolecular functionalities on graphene for the development various biosensing platform. Lu *et al*¹⁸² used cyclodextrin functionalized graphene and adamantane-modified horseradish peroxidase (HRP) for the construction of hydrogen peroxide (H₂O₂) biosensor. Cyclodextrin can form a stable host-guest inclusion complex by binding various organic and biological molecules into its cavities with high selectivity^{183,184}. The supramolecular recognition capability of the CD was combined with highly conductive RGO to improve the electrochemical activity. Detailed structural analysis proved that HRP retained its structure and activity by implying the good biocompatibility of cyclodextrin-functionalized graphene¹⁸⁵. The resulting biosensor showed a wide linear range, long-term stability, good repeatability and high sensitivity to H₂O₂ sensing with the detection limit of 0.1 mM.

Palanisamy *et al*¹⁸⁶ had developed a glucose biosensor based on direct electrochemistry of glucose oxidase (GOx) immobilized on the reduced graphene oxide (RGO) and β-cyclodextrin (CD) nanocomposite. They had used β-cyclodextrin (CD) as a biocompatible material with RGO to load the GOx enzyme (Fig. 1.25). The hydrophilic outer surface and hydrophobic inner cavity of CD provided a suitable environment for the immobilization of redox active enzymes or proteins. The fabricated biosensor showed direct electrochemistry of GOx with a good sensitivity for glucose sensing.

Zhao *et al*¹⁸⁷ reported a novel ultrasensitive biosensing platform based on a electrochemically reduced graphene oxide (ERGO)-Au nanoparticles (AuNPs)-β-cyclodextrin (β-CD)- Prussian blue-chitosan (PB-CS) with acetylcholinesterase (AChE) to detect organophosphorus pesticides (OPs). The resulting biosensor exhibited excellent sensitivity, good stability, fast electrochemical response and good reproducibility for the detection of malathion and carbaryl.

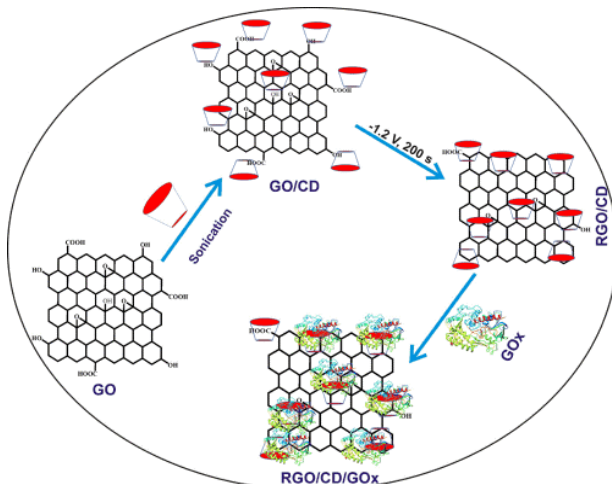


FIGURE 1.25

A schematic representation for the fabrication of RGO/CD composite and construction of glucose biosensor. (Reproduced from ref.¹⁸⁶ with permission copyright © 2015 WILEY-VCH Verlag GmbH & Co. KGaA, Weinheim)

Non-enzymatic biosensors

Although enzyme based biosensors are the most popular one, they have their few significant drawbacks including their low operational stability (denaturation and digestion), sensitivity to environmental conditions, difficulties in repeatable use, and high costs in preparation and purification^{188,189}. To overcome these aforementioned limitations, non-enzymatic biosensors have been proven as low-cost and highly stable alternatives to natural enzymes. In recent years, design of biomimetic non-enzymatic biosensors has very rapidly emerged as a lively field of research. Supramolecular functionalities on graphene also exhibited some promising results for development of non-enzymatic biosensors^{190,191}.

De *et al*¹⁹² reported a non-enzymatic cholesterol detection approach using chemically converted graphene modified with β -CD. Methylene Blue (MB) acted as a redox indicator in this process, which forms an inclusion complex with β -CD and acts as a cholesterol sensing matrix (Fig. 1.26). The MB molecule is replaced by cholesterol molecule and goes into the buffer solution, which is electrochemically detected using DPV technique. This sensing platform can efficiently detect cholesterol in the micro molar concentration range with good selectivity over the common interfering species. Li *et al*¹⁹³ also reported a similar electrochemical approach for non-enzymatic cholesterol sensing based on a competitive host–guest recognition between β -cyclodextrin (β -CD) and a signal probe (methylene blue)/target molecule using a β -CD/poly(N-acetylaniline)/graphene modified electrode. The resulting sensor also used DPV technique and obtained a linear response range of 1.00 to 50.00 mM for cholesterol with a low detection limit of 0.5 mM. Jana *et al*¹⁹⁴ also established a fluorescence based cholesterol detection method using competitive host–guest interaction between graphene bound β -cyclodextrin with rhodamine 6G (R6G) and cholesterol. In this system, the fluorescence of R6G is quenched by graphene but is ‘turned on’ as it substituted by cholesterol from the β -CD host. This method can achieve the detection limit up to the nanomolar concentration range.

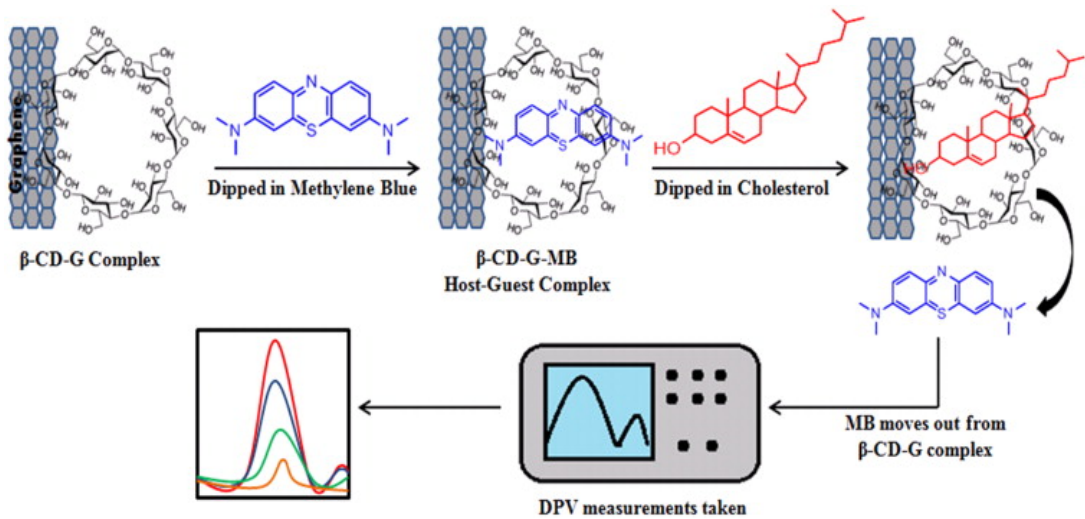


FIGURE 1.26

A schematic representation for the mechanism of cholesterol sensing, using Grp-β-CD as the working matrix. (Reproduced from ref.¹⁹² with permission Copyright © 2015 Elsevier B.V.)

Antibody and aptamer based biosensors

An antibody is consisted of many individual amino acids organized in a highly ordered sequence. Moreover, every antibody fits its unique antigen in a highly specific way. This unique recognition property is extremely important for development of antibody-based immunosensors where only the specific analyte (the antigen) fits into the antibody binding site¹⁸¹. Aptamers are artificial single-stranded DNA or RNA oligonucleotides (typically <100mer), which can be used for precisely bind with various target molecules (e.g. proteins, cells, viruses, bacteria, and small molecules such as organic dyes, metal ions)¹⁸¹. Aptamers are equivalent to monoclonal antibodies regarding their binding affinities and they are more resilient to denaturation and degradation. The properties of aptamers such as binding affinities and specificities can also be modified by means of rational design or by techniques of molecular evolution. Mainly, for all these versatile properties, they can be used for the development of a new generation biosensors.

Wei *et al*¹⁹⁵ reported a novel immunoassay for ultrasensitive electrochemical detection of carcino-embryonic antigen (CEA) using host-guest interaction of β-cyclodextrin functionalized graphene and Cu@Ag core-shell nanoparticles with adamantane-modified antibody. The designed immunosensor showed excellent sensing performance for the measurement of CEA with wide linear range of 0.0001– 20 ng/mL, low detection limit (20 fg/mL), high sensitivity, reproducibility and stability, which introduced a promising application prospect in clinical diagnostics. Guo *et al*¹⁹⁶ demonstrated a facile one-pot controlled synthesis of thio-β-cyclodextrin functionalized graphene/gold nanoparticles for the development of electrochemical thrombin aptasensor. The as synthesized nanocomposite possessed excellent electrical properties and large surface area of graphene and AuNPs combined with supramolecular recognition capacity of β-cyclodextrin (Fig. 1.27). This biosensor displayed a wide linear range for thrombin detection from 1.6×10^{-17} M to 8.0×10^{-15} M and a lower limit of detection 5.2×10^{-18} M. Wang *et al*¹⁹⁷ also derived a β-Cyclodextrin functionalized graphene as a highly conductive and multi-site platform for DNA immobilization and ultrasensitive biosensor. Yuan *et al*¹⁹⁸ designed a supramolecular assembly of perylene derivatives

on Au functionalized graphene based electrochemiluminescent-immunosensor for cancer biomarker detection. The immunosensor showed an extensive dynamic range of $0.001\text{--}10\text{ ng mL}^{-1}$ and detection limits of 0.3 pg mL^{-1} , respectively. In another work, Yuan *et al*¹⁹⁹ developed a novel electrochemical aptasensor for ultrasensitive detection of thrombin by using conductive graphene-3,4,9,10-perylenetetracarboxylic dianhydride nanocomposites as a sensing platform and hollow PtCo nanochains–thionine–Pt–HRP labeled secondary thrombin aptamer for signal amplification. This amplification approach exhibited good stability and reproducibility and high sensitivity, which could provide a promising potential for clinical diagnostics.

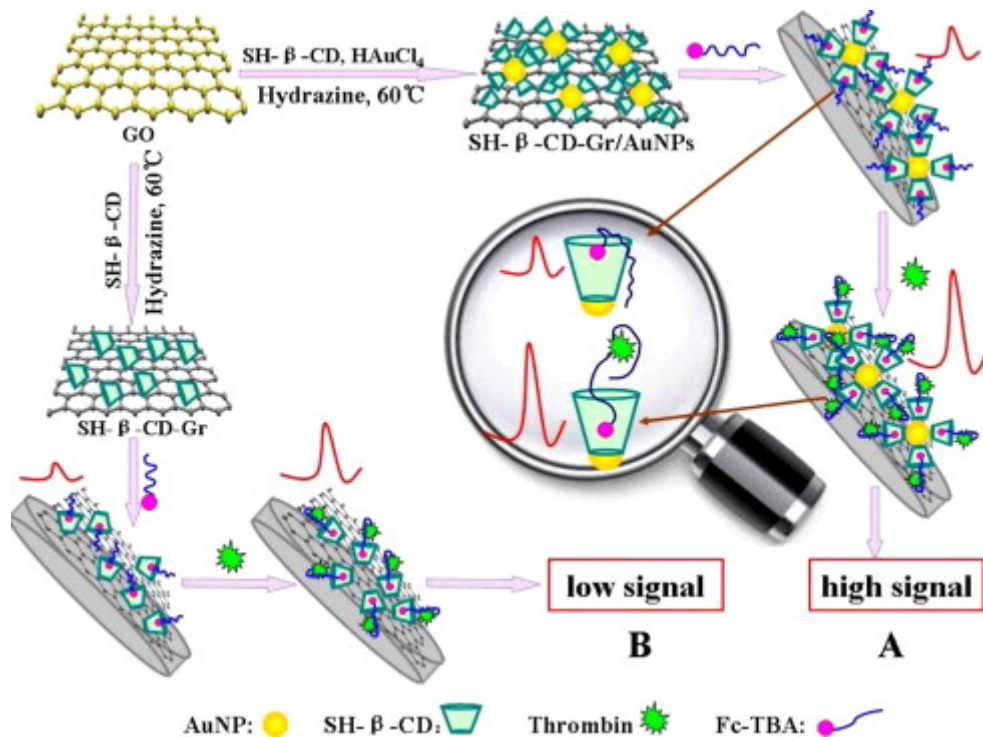


FIGURE 1.27

Schematic procedure for the synthesis of SH-β-CD-Gr/AuNPs and the electrochemical thrombin detection by the use of SH-β-CD-Gr/AuNPs with higher supramolecular recognition ability (A) than SH-β-CD-Gr (B). (Reproduced from ref.¹⁹⁶ with permission Copyright © 2015 Elsevier B.V.)

Concluding remarks and outlook

In recent years the development of graphene based sensors and biosensors have been tremendous, the electronic properties of graphene combined with its high surface area make it an ideal candidate as a transducer for sensors. Moreover, RGO and especially CMG provide further benefits in the form of significantly lowered production cost and the possibility of up scaling. Furthermore, the residual functional group and especially introduced functionalization provide unique possibility increasing selectivity of these systems. In this chapter, we have discussed properties of graphene and related 2D carbon materials. How these can be synthesized,

functionalized and characterized. We have focus on how supramolecular moieties can be used to great benefit to introduce crucial selectivity to sensor systems whether by limiting access to the electrode surface or by utilizing competitive binding to release probe molecules upon detection of target analytes. Finally, we discussed the possibility of using supramolecules as anchors for biomolecules such as enzymes, antibodies and aptasensors for highly specific detection of important biological relevant compounds. However it should be noted that, despite many impressive examples that have been demonstrated in this area, the full potential has not been explored likewise many new questions and challenges have been raised. With covalent functionalization of graphene with highly specific ionophores or presently available supramolecular recognition systems, it is possible that highly sensitive sensors with ultra-high selectivity can be constructed, either in the form of electrochemical sensors or by competitive exchange of dyes to form optical sensors. The work with anchoring biomolecules through supramolecular complexation provides a feasible method of fabricating new biosensors where biomolecules can be attached regardless of isoelectric point, hydrophobicity or other variable properties of target receptor biomolecules.

References

1. Lax, A.; Rchme, F.; Maxwell, R. *Natl. Trust Annu. Archaeol. Rev.* **1998**, 18–23.
2. Palermo, V. *Chem. Commun. (Camb).* **2013**, 49 (28), 2848–2857.
3. Wallace, P. R. *Phys. Rev.* **1947**, 71, 622–634.
4. McClure, J. W. *Phys. Rev.* **1956**, 104, 666–671.
5. Slonczewski, J.; Weiss, P. *Phys. Rev.* **1958**, 109 (2), 272–279.
6. Mermin, N. D. *Phys. Rev.* **1968**, 176, 250–254.
7. Fradkin, E. *Phys. Rev. B* **1986**, 33 (5), 3263–3268.
8. Geim, A. K.; Novoselov, K. S. *Nat Mater* **2007**, 6 (3), 183–191.
9. Novoselov, K. S.; Geim, A. K.; Morozov, S. V.; Jiang, D.; Zhang, Y.; Dubonos, S. V.; Grigorieva, I. V.; Firsov, A. A.; K.S. Novoselov1, A.K. Geim1, S.V. Morozov2, D. Jiang1, Y. Zhang1, S.V. Dubonos2, I.V. Grigorieva1, a. a. F.; Using, K. *Science (80-.)*. **2004**, 306 (5696), 666–669.
10. Novoselov, K. S.; Jiang, D.; Schedin, F.; Booth, T. J.; Khotkevich, V. V.; Morozov, S. V.; Geim, a K. *Proc. Natl. Acad. Sci. U. S. A.* **2005**, 102 (30), 10451–10453.
11. Novoselov, K. S.; Geim, A. K.; Morozov, S. V.; Jiang, D.; Katsnelson, M. I.; Grigorieva, I. V.; Dubonos, S. V.; Firsov, A. A. *Nature* **2005**, 438 (7065), 197–200.
12. Nobelprize.org. The Nobel Prize in Physics 2010.
13. Peigney, A.; Laurent, C.; Flahaut, E.; Bacsá, R. R.; Rousset, A. *Carbon N. Y.* **2001**, 39, 507–514.
14. Nair, R. R.; Grigorenko, A. N.; Blake, P.; Novoselov, K. S.; Booth, T. J.; Peres, N. M. R.; Stauber, T.; Geim, A. K. *Science (80-.)*. **2008**, 320 (5881), 1308.
15. Lee, C.; Wei, X.; Kysar, J. W.; Hone, J. *Sci.* **2008**, 321 (5887), 385–388.
16. Balandin, A. A.; Ghosh, S.; Bao, W.; Calizo, I.; Teweldebrhan, D.; Miao, F.; Lau, C. N. *Nano Lett.* **2008**, 8 (3), 902–907.

17. Seol, J. H.; Jo, I.; Moore, A. L.; Lindsay, L.; Aitken, Z. H.; Pettes, M. T.; Li, X.; Yao, Z.; Huang, R.; Broido, D.; Mingo, N.; Ruoff, R. S.; Shi, L. *Science* (80-.). **2010**, *328* (5975), 213–216.
18. Bolotin, K. I.; Sikes, K. J.; Jiang, Z.; Klima, M.; Fudenberg, G.; Hone, J.; Kim, P.; Stormer, H. L. *Solid State Commun.* **2008**, *146* (9-10), 351–355.
19. Zhang, Y.; Tan, Y. W.; Stormer, H. L.; Kim, P. *Nature* **2005**, *438* (7065), 201–204.
20. K.S. Novoselov, A.K. Geim, S.V. Morozov, D. Jiang, Y. Zhang, S.V. Dubonos, I.V. Grigorieva, a. a. F.; Jiang, Z.; Zhang, Y.; Morozov, S. V.; Stormer, H. L.; Zeitler, U.; Maan, J. C.; Boebinger, G. S.; Kim, P.; Geim, A. K. *Science* (80-.). **2007**, *315* (March), 2007.
21. Robinson, J.; Weng, X.; Trumbull, K.; Cavalero, R.; Wetherington, M.; Frantz, E.; LaBella, M.; Hughes, Z.; Fanton, M.; Snyder, D. *ACS Nano* **2010**, *4* (1), 153–158.
22. Muñoz, R.; Gómez-Aleixandre, C. *Chem. Vap. Depos.* **2013**, *19* (10-11-12), 297–322.
23. Seah, C.-M.; Chai, S.-P.; Mohamed, A. R. *Carbon N. Y.* **2014**, *70*, 1–21.
24. Li, X.; Cai, W.; Colombo, L.; Ruoff, R. S. *Nano Lett.* **2009**, *9* (12), 4268–4272.
25. Li, X.; Magnuson, C. W.; Venugopal, A.; An, J.; Suk, J. W.; Han, B.; Borysiak, M.; Cai, W.; Velamakanni, A.; Zhu, Y.; Fu, L.; Vogel, E. M.; Voelkl, E.; Colombo, L.; Ruoff, R. S. *Nano Lett.* **2010**, *10* (11), 4328–4334.
26. Li, X.; Magnuson, C. W.; Venugopal, A.; Tromp, R. M.; Hannon, J. B.; Vogel, E. M.; Colombo, L.; Ruoff, R. S. *J. Am. Chem. Soc.* **2011**, *133* (9), 2816–2819.
27. Zhang, Y.; Gomez, L.; Ishikawa, F. N.; Madaria, A.; Ryu, K.; Wang, C.; Badmaev, A.; Zhou, C. *J. Phys. Chem. Lett.* **2010**, *1* (20), 3101–3107.
28. Momiuchi, Y.; Yamada, K.; Kato, H.; Homma, Y.; Hibino, H.; Odahara, G.; Oshima, C. *J. Phys. D. Appl. Phys.* **2014**, *47* (45), 455301.
29. Shu, H.; Chen, X.; Tao, X.; Ding, F. *ACS Nano* **2012**, *6* (4), 3243–3250.
30. Lahiri, J.; Miller, T.; Adamska, L.; Oleynik, I. I.; Batzill, M. *Nano Lett.* **2010**, *11* (2), 518–522.
31. Mittendorfer, F.; Garhofer, A.; Redinger, J.; Klimeš, J.; Harl, J.; Kresse, G. *Phys. Rev. B* **2011**, *84* (20), 201401.
32. Bae, S.; Kim, H.; Lee, Y.; Xu, X.; Park, J.-S.; Zheng, Y.; Balakrishnan, J.; Lei, T.; Kim, H. R.; Song, Y. Il; Kim, Y.-J.; Kim, K. S.; Ozyilmaz, B.; Ahn, J.-H.; Hong, B. H.; Iijima, S. *Nat. Nanotechnol.* **2010**, *5* (8), 574–578.
33. Hu, B.; Ago, H.; Orofeo, C. M.; Ogawa, Y.; Tsuji, M. *New J. Chem.* **2012**, *36* (1), 73.
34. Seifert, M.; Vargas, J. E. B.; Bobinger, M.; Sachsenhauser, M.; Cummings, A. W.; Roche, S.; Garrido, J. A. *2D Mater.* **2015**, *2* (2), 024008.
35. Yazyev, O. V.; Louie, S. G. *Nat. Mater.* **2010**, *9* (10), 806–809.
36. Yazyev, O. V.; Chen, Y. P. *Nat. Nanotechnol.* **2014**, *9* (10), 755–767.
37. Wang, Y.; Zheng, Y.; Xu, X.; Dubuisson, E.; Bao, Q.; Lu, J.; Loh, K. P. *ACS Nano* **2011**, *5* (12), 9927–9933.
38. Gorantla, S.; Bachmatiuk, A.; Hwang, J.; Alsalman, H. a; Kwak, J. Y.; Seyller, T.; Eckert, J.; Spencer, M. G.; Rummeli, M. H. *Nanoscale* **2014**, *6* (2), 889–896.
39. Israelachvili, J. N. *Intermolecular and Surface Forces*, Third edit.; Academic Press: Waltham, 2011.

40. Pierson, H. O. In *Handbook of Carbon, Graphite, Diamonds and Fullerenes*; Noyes Publications Inc.: New Jersey, 1993; pp 43–69.
41. Hernandez, Y.; Nicolosi, V.; Lotya, M.; Blighe, F. M.; Sun, Z.; De, S.; McGovern, I. T.; Holland, B.; Byrne, M.; Gun'Ko, Y. K.; Boland, J. J.; Niraj, P.; Duesberg, G.; Krishnamurthy, S.; Goodhue, R.; Hutchison, J.; Scardaci, V.; Ferrari, A. C.; Coleman, J. N. *Nat. Nanotechnol.* **2008**, *3* (9), 563–568.
42. Kahl, H.; Wadewitz, T.; Winkelmann, J. *J. Chem. Eng. Data* **2003**, *48*, 580–586.
43. Singh, M. *Phys. Chem. Liq.* **2006**, *44* (5), 579–584.
44. Coleman, J. N. *Acc. Chem. Res.* **2013**, *46* (1), 14–22.
45. Khan, U.; Porwal, H.; Óneill, A.; Nawaz, K.; May, P.; Coleman, J. N. *Langmuir* **2011**, *27* (15), 9077–9082.
46. Solomon, H. M.; Burgess, B. A.; Kennedy, G. L.; Staples, R. E. *Drug Chem. Toxicol.* **1995**, *18* (4), 271–293.
47. Kennedy, G. L.; Sherman, H. *Drug Chem. Toxicol.* **1986**, *9* (2), 147–170.
48. Jasper, J. J. *J. Phys. Chem. Ref. Data* **1972**, *1* (4), 841.
49. Ciesielski, A.; Samorì, P. *Chem. Soc. Rev.* **2014**, *43* (1), 381–398.
50. Parviz, D.; Das, S.; Ahmed, H. S. T.; Irin, F.; Bhattacharia, S.; Green, M. J. *ACS Nano* **2012**, *6* (10), 8857–8867.
51. Khan, U.; O'Neill, A.; Porwal, H.; May, P.; Nawaz, K.; Coleman, J. N. *Carbon N. Y.* **2012**, *50* (2), 470–475.
52. Gong, L.; Kinloch, I. A.; Young, R. J.; Riaz, I.; Jalil, R.; Novoselov, K. S. *Adv. Mater.* **2010**, *22* (24), 2694–2697.
53. Green, A. A.; Hersam, M. C. *Nano Lett.* **2009**, *9* (12), 4031–4036.
54. Brodie, B. C. *Philos. Trans. R. Soc. London* **1859**, *149*, 249–259.
55. Staudenmaier, L. *Berichte der Dtsch. Chem. Gesellschaft* **1898**, *31* (2), 1481–1487.
56. Hummers, W. S. J.; Offeman, R. E. *J. Am. Chem. Soc.* **1958**, *80* (6), 1339–1339.
57. Jung, I.; Dikin, D. a.; Piner, R. D.; Ruoff, R. S. *Nano Lett.* **2008**, *8* (12), 4283–4287.
58. Lerf, A.; He, H.; Riedl, T.; Forster, M.; Klinowski, J. *Solid State Ionics* **1997**, *101-103*, 857–862.
59. Buchsteiner, A.; Lerf, A.; Pieper, J. *J. Phys. Chem. B* **2006**, *110* (45), 22328–22338.
60. Szabó, T.; Tombácz, E.; Illés, E.; Dékány, I. *Carbon N. Y.* **2006**, *44* (3), 537–545.
61. Paredes, J. I.; Villar-Rodil, S.; Martiñez-Alonso, A.; Tascoñ, J. M. D. *Langmuir* **2008**, *24* (19), 10560–10564.
62. Dreyer, D. R.; Park, S.; Bielawski, C. W.; Ruoff, R. S. *Chem. Soc. Rev.* **2010**, *39* (1), 228–240.
63. Dimiev, A.; Kosynkin, D. V.; Alemany, L. B.; Chaguine, P.; Tour, J. M. *J. Am. Chem. Soc.* **2012**, *134* (5), 2815–2822.
64. Hofmann, U.; Holst, R. *Berichte der Dtsch. Chem. Gesellschaft* **1939**, *72* (4), 754–771.
65. Scholz, W.; Boehm, H. P. *Z. anorg. allg. Chem.* **1969**, *369* (1967), 327–340.
66. Nakajima, T.; Mabuchi, a.; Hagiwara, R. *Carbon N. Y.* **1988**, *26* (3), 357–361.
67. Lerf, A.; He, H.; Forster, M.; Klinowski, J. **1998**, *5647* (97), 4477–4482.
68. He, H.; Klinowski, J.; Forster, M.; Lerf, A. *Chem. Phys. Lett.* **1998**, *287* (1-2), 53–56.

69. He, H.; Riedl, T.; Lerf, A.; Klinowski, J. *J. Phys. Chem.* **1996**, *100* (51), 19954–19958.
70. Zhu, Y.; Murali, S.; Cai, W.; Li, X.; Suk, J. W.; Potts, J. R.; Ruoff, R. S. *Adv. Mater.* **2010**, *22* (35), 3906–3924.
71. Stankovich, S.; Dikin, D. A.; Piner, R. D.; Kohlhaas, K. A.; Kleinhammes, A.; Jia, Y.; Wu, Y.; Nguyen, S. T.; Ruoff, R. S. *Carbon N. Y.* **2007**, *45* (7), 1558–1565.
72. Shin, H.-J.; Kim, K. K.; Benayad, A.; Yoon, S.-M.; Park, H. K.; Jung, I.-S.; Jin, M. H.; Jeong, H.-K.; Kim, J. M.; Choi, J.-Y.; Lee, Y. H. *Adv. Funct. Mater.* **2009**, *19* (12), 1987–1992.
73. Thakur, S.; Karak, N. *Carbon N. Y.* **2015**, *94* (June), 224–242.
74. Chua, C. K.; Pumera, M. *Chem Soc Rev* **2014**, *43* (1), 291–312.
75. Zhang, J.; Yang, H.; Shen, G.; Cheng, P. **2010**, 1112–1114.
76. Gao, J.; Liu, F.; Liu, Y.; Ma, N.; Wang, Z.; Zhang, X. *Chem. Mater.* **2010**, *22*, 2213–2218.
77. Mei, X.; Ouyang, J. *Carbon N. Y.* **2011**, *49* (15), 5389–5397.
78. Fan, Z.-J.; Kai, W.; Yan, J.; Wei, T.; Zhi, L.-J.; Feng, J.; Ren, Y.; Song, L.-P.; Wei, F. *ACS Nano* **2011**, *5* (1), 191–198.
79. Fan, B. X.; Peng, W.; Li, Y.; Li, X.; Wang, S.; Zhang, G. *Adv. Mater.* **2008**, *20*, 4490–4493.
80. Mcallister, M. J.; Li, J.; Adamson, D. H.; Schniepp, H. C.; Abdala, A. a; Liu, J.; Herrera-alonso, O. M.; Milius, D. L.; Car, R.; Prud, R. K.; Aksay, I. a. *Chem. Mater.* **2007**, *19* (4), 4396–4404.
81. Kudin, K. N.; Ozbas, B.; Schniepp, H. C.; Prud’Homme, R. K.; Aksay, I. a; Car, R. *Nano Lett.* **2008**, *8* (1), 36–41.
82. Schniepp, H. C.; Li, J. L.; McAllister, M. J.; Sai, H.; Herrera-Alonson, M.; Adamson, D. H.; Prud’homme, R. K.; Car, R.; Seville, D. a.; Aksay, I. a. *J. Phys. Chem. B* **2006**, *110* (17), 8535–8539.
83. Sundaram, R. S.; Gómez-Navarro, C.; Balasubramanian, K.; Burghard, M.; Kern, K. *Adv. Mater.* **2008**, *20* (16), 3050–3053.
84. Zhou, M.; Wang, Y.; Zhai, Y.; Zhai, J.; Ren, W.; Wang, F.; Dong, S. *Chem. - A Eur. J.* **2009**, *15* (25), 6116–6120.
85. Georgakilas, V.; Otyepka, M.; Bourlinos, A. B.; Chandra, V.; Kim, N.; Kemp, K. C.; Hobza, P.; Zboril, R.; Kim, K. S. *Chem. Rev.* **2012**, *112* (11), 6156–6214.
86. Wang, Y.; Shao, Y.; Matson, D. W.; Li, J.; Lin, Y. *4* (4).
87. Long, B.; Manning, M.; Burke, M.; Szafranek, B. N.; Visimberga, G.; Thompson, D.; Greer, J. C.; Povey, I. M.; MacHale, J.; Lejosne, G.; Neumaier, D.; Quinn, A. J. *Adv. Funct. Mater.* **2012**, *22* (4), 717–725.
88. Hu, H.; Xin, J. H.; Hu, H.; Wang, X.; Kong, Y. *Appl. Catal. A Gen.* **2015**, *492*, 1–9.
89. Shi, G.; Wang, X. *Phys. Chem. Chem. Phys.* **2015**, *17*, 28484–28504.
90. Jia, X.; Campos-Delgado, J.; Terrones, M.; Meunier, V.; Dresselhaus, M. S. *Nanoscale* **2011**, *3* (1), 86–95.
91. Lu, Y. H.; Wu, R. Q.; Shen, L.; Yang, M.; Sha, Z. D.; Cai, Y. Q.; He, P. M.; Feng, Y. P. *Appl. Phys. Lett.* **2009**, *94* (12), 3–5.
92. Enoki, T.; Takai, K. *Solid State Commun.* **2009**, *149* (27–28), 1144–1150.
93. Quintana, M.; Montellano, A.; Del Rio Castillo, A. E.; Tendeloo, G. Van; Bittencourt, C.; Prato, M. *Chem. Commun. (Camb).* **2011**, *47* (33), 9330–9332.

94. Sun, Z.; Kohama, S. I.; Zhang, Z.; Lomeda, J. R.; Tour, J. M. *Nano Res.* **2010**, *3* (2), 117–125.
95. Bekyarova, E.; Itkis, M. E.; Ramesh, P.; Berger, C.; Sprinkle, M.; De Heer, W. a.; Haddon, R. C. *J. Am. Chem. Soc.* **2009**, *131* (4), 1336–1337.
96. Bettinger, H. F. *Chemistry* **2006**, *12* (16), 4372–4379.
97. Chua, C. K.; Ambrosi, A.; Pumera, M. *Chem. Commun. (Camb)*. **2012**, *48* (43), 5376–5378.
98. Liu, L.-H.; Yan, M. *J. Mater. Chem.* **2011**, *21*, 3273.
99. Strom, T. A.; Dillon, E. P.; Hamilton, C. E.; Barron, A. R. *Chem. Commun. (Camb)*. **2010**, *46* (23), 4097–4099.
100. Quintana, M.; Spyrou, K.; Grzelczak, M.; Browne, W. R.; Rudolf, P.; Prato, M. *ACS Nano* **2010**, *4* (6), 3527–3533.
101. Zhang, X.; Hou, L.; Cnossen, A.; Coleman, A. C.; Ivashenko, O.; Rudolf, P.; Van Wees, B. J.; Browne, W. R.; Feringa, B. L. *Chem. - A Eur. J.* **2011**, *17* (32), 8957–8964.
102. Ragoussi, M. E.; Malig, J.; Katsukis, G.; Butz, B.; Spiecker, E.; De La Torre, G.; Torres, T.; Guldi, D. M. *Angew. Chemie - Int. Ed.* **2012**, *51* (26), 6421–6425.
103. Sarkar, S.; Bekyarova, E.; Haddon, R. C. *Acc. Chem. Res.* **2012**, *45* (4), 673–682.
104. Sarkar, S.; Bekyarova, E.; Niyogi, S.; Haddon, R. C. *J. Am. Chem. Soc.* **2011**, *133* (10), 3324–3327.
105. Dreyer, D. R.; Todd, A. D.; Bielawski, C. W. *Chem. Soc. Rev.* **2014**, *43* (15), 5288.
106. Niyogi, S.; Bekyarova, E.; Itkis, M. E.; McWilliams, J. L.; Hamon, M. a; Haddon, R. C. *J. Am. Chem. Soc.* **2006**, *128* (24), 7720–7721.
107. Su, P.-G.; Lu, Z.-M. *Sensors Actuators B Chem.* **2015**, *211*, 157–163.
108. Chen, H. J.; Zhang, Z. H.; Cai, R.; Chen, X.; Liu, Y. N.; Rao, W.; Yao, S. Z. *Talanta* **2013**, *115*, 222–227.
109. Yang, H.; Shan, C.; Li, F.; Han, D.; Zhang, Q.; Niu, L. *Chem. Commun. (Camb)*. **2009**, No. 26, 3880–3882.
110. Shan, C.; Yang, H.; Han, D.; Zhang, Q.; Ivaska, A.; Niu, L. *Langmuir* **2009**, *25* (20), 12030–12033.
111. Stankovich, S.; Piner, R. D.; Nguyen, S. T.; Ruoff, R. S. *Carbon N. Y.* **2006**, *44* (15), 3342–3347.
112. Yang, H.; Shan, C.; Li, F.; Han, D.; Zhang, Q.; Niu, L. *Chem. Commun.* **2009**, No. 26, 3880–3882.
113. Lomeda, J. R.; Doyle, C. D.; Kosynkin, D. V.; Hwang, W.-F.; Tour, J. M. *J. Am. Chem. Soc.* **2008**, *130* (48), 16201–16206.
114. Ismaili, H.; Geng, D.; Sun, A. X.; Kantzas, T. T.; Workentin, M. S. *Langmuir* **2011**, *27* (21), 13261–13268.
115. Hsiao, M.-C.; Liao, S.-H.; Yen, M.-Y.; Liu, P.-I.; Pu, N.-W.; Wang, C.-A.; Ma, C.-C. *M. ACS Appl. Mater. Interfaces* **2010**, *2* (11), 3092–3099.
116. Haubner, K.; Murawski, J.; Olk, P.; Eng, L. M.; Ziegler, C.; Adolphi, B.; Jaehne, E. *ChemPhysChem* **2010**, *11*, 2131–2139.
117. Szabó, T.; Berkesi, O.; Forgó, P.; Josepovits, K.; Sanakis, Y.; Petridis, D.; Dékány, I. *Chem. Mater.* **2006**, *18* (11), 2740–2749.

118. Gómez-Navarro, C.; Meyer, J. C.; Sundaram, R. S.; Chuvilin, A.; Kurasch, S.; Burghard, M.; Kern, K.; Kaiser, U. *Nano Lett.* **2010**, *10* (4), 1144–1148.
119. Liu, Y.; Weinert, M.; Li, L. *Nanotechnology* **2015**, *26* (3), 035702.
120. Dreyer, D. R.; Park, S.; Bielawski, C. W.; Ruoff, R. S. *Chem. Soc. Rev.* **2010**, *39* (1), 228–240.
121. Rozada, R.; Paredes, J. I.; López, M. J.; Villar-Rodil, S.; Cabria, I.; Alonso, J. A.; Martínez-Alonso, A.; Tascón, J. M. D. *Nanoscale* **2015**, *7* (6), 2374–2390.
122. Wang, Z.; Dong, Y.; Li, H.; Zhao, Z.; Bin Wu, H.; Hao, C.; Liu, S.; Qiu, J.; Lou, X. W. (David). *Nat. Commun.* **2014**, *5* (May), 5002.
123. Kumar, B.; Asadi, M.; Pisasale, D.; Sinha-Ray, S.; Rosen, B. A.; Haasch, R.; Abiade, J.; Yarin, A. L.; Salehi-Khojin, A. *Nat. Commun.* **2013**, *4*, 1–8.
124. Wang, J. *Biosens. Bioelectron.* **2006**, *21* (10), 1887–1892.
125. Sanghavi, B. J.; Sitaula, S.; Griep, M. H.; Karna, S. P.; Ali, M. F.; Swami, N. S. *Anal. Chem.* **2013**, *85* (17), 8158–8165.
126. Suslick, K. S. *MRS Bull.* **2004**, *29* (10), 720–725.
127. Moos, R.; Izu, N.; Rettig, F.; Reiß, S.; Shin, W.; Matsubara, I. *Sensors* **2011**, *11* (12), 3439–3465.
128. Fu, X.; Benson, R. F.; Wang, J.; Fries, D. *Sensors Actuators B Chem.* **2005**, *106* (1), 296–301.
129. Burnworth, M.; Rowan, S. J.; Weder, C. *Chemistry* **2007**, *13*, 7828–7836.
130. Xia, F.; Zuo, X.; Yang, R.; Xiao, Y.; Kang, D.; Vallee-Belisle, A.; Gong, X.; Yuen, J. D.; Hsu, B. B. Y.; Heeger, A. J.; Plaxco, K. W. *Proc. Natl. Acad. Sci.* **2010**, *107* (24), 10837–10841.
131. Nolan, E. M.; Lippard, S. J. *J. Am. Chem. Soc.* **2003**, *125* (47), 14270–14271.
132. Ghosn, M. W.; Wolf, C. *Tetrahedron* **2011**, *67* (36), 6799–6803.
133. Li, X.-G.; Feng, H.; Huang, M.-R.; Gu, G.-L.; Moloney, M. G. *Anal. Chem.* **2012**, *84* (1), 134–140.
134. Dey, R. S.; Raj, C. R. *J. Phys. Chem. C* **2010**, *114* (49), 21427–21433.
135. Chen, Q.; Zhu, L.; Zhao, C.; Wang, Q.; Zheng, J. *Adv. Mater.* **2013**, *25* (30), 4171–4176.
136. You, L.; Zha, D.; Anslyn, E. V. *Chem. Rev.* **2015**, *115* (15), 7840–7892.
137. Sun, R.; Wang, L.; Yu, H.; Abdin, Z.; Chen, Y.; Huang, J.; Tong, R. *Organometallics* **2014**.
138. Rajagopal, S.; Rajagopal, K.; Lefkowitz, R. J. *Nat. Rev. Drug Discov.* **2010**, *9* (5), 373–386.
139. Litman, G. W.; Rast, J. P.; Shablott, M. J.; Haire, R. N.; Hulst, M.; Roess, W.; Litman, R. T.; Hinds-Frey, K. R.; Zilch, a; Amemiya, C. T. *Mol. Biol. Evol.* **1993**, *10* (1), 60–72.
140. Chen, L.; Xu, S.; Li, J. *Chem. Soc. Rev.* **2011**, *40* (5), 2922.
141. Zhan, B.; Li, C.; Yang, J.; Jenkins, G.; Huang, W.; Dong, X. *Small* **2014**, *10* (20), 4042–4065.
142. Trung, T. Q.; Tien, N. T.; Kim, D.; Jang, M.; Yoon, O. J.; Lee, N.-E. *Adv. Funct. Mater.* **2014**, *24* (1), 117–124.
143. Lu, G.; Ocola, L. E.; Chen, J. *Nanotechnology* **2009**, *20* (44), 445502.
144. Yoshio, M.; Noguchi, H. *Anal. Lett.* **1982**, *15* (15), 1197–1276.
145. Dalapati, S.; Jana, S.; Guchhait, N. *Spectrochim. Acta - Part A Mol. Biomol. Spectrosc.* **2014**, *129* (APRIL 2014), 499–508.
146. Bühlmann, P.; Pretsch, E.; Bakker, E. *Chem. Rev.* **1998**, *98* (4), 1593–1688.
147. Bakker, E. *Anal. Chem.* **2004**, *76* (12), 3285–3298.

148. Bakker, E.; Pretsch, E.; Bühlmann, P. *Anal. Chem.* **2000**, *72* (6), 1127–1133.
149. Maehashi, K.; Sofue, Y.; Okamoto, S.; Ohno, Y.; Inoue, K.; Matsumoto, K. *Sensors Actuators, B Chem.* **2013**, *187*, 45–49.
150. Abraham, A. A.; Rezayi, M.; Manan, N. S. A.; Narimani, L.; Rosli, A. N. Bin; Alias, Y. *Electrochim. Acta* **2015**, *165*, 221–231.
151. Li, F.; Ye, J.; Zhou, M.; Gan, S.; Zhang, Q.; Han, D.; Niu, L. *Analyst* **2012**, *137* (3), 618–623.
152. Jaworska, E.; Lewandowski, W.; Mieczkowski, J.; Maksymiuk, K.; Michalska, A. *Analyst* **2013**, *138* (8), 2363–2371.
153. Hernández, R.; Riu, J.; Bobacka, J.; Vallés, C.; Jiménez, P.; Benito, A. M.; Maser, W. K.; Rius, F. X. *J. Phys. Chem. C* **2012**, *116* (42), 22570–22578.
154. Afkhami, A.; Shirzadmehr, A.; Madrakian, T.; Bagheri, H. *Talanta* **2015**, *131*, 548–555.
155. Olsen, G.; Ulstrup, J.; Chi, Q. *ACS Appl. Mater. Interfaces* **2015**, acsami.5b11597.
156. Gramage-Doria, R.; Armspach, D.; Matt, D. *Coord. Chem. Rev.* **2013**, *257* (3–4), 776–816.
157. Sambrook, M. R.; Notman, S. *Chem. Soc. Rev.* **2013**, *42* (24), 9251–9267.
158. Pinalli, R.; Suman, M.; Dalcanale, E. *European J. Org. Chem.* **2004**, *2004* (3), 451–462.
159. Wu, S.; Lan, X.; Cui, L.; Zhang, L.; Tao, S.; Wang, H.; Han, M.; Liu, Z.; Meng, C. *Anal. Chim. Acta* **2011**, *699* (2), 170–176.
160. Guo, Y.; Guo, S.; Li, J.; Wang, E.; Dong, S. *Talanta* **2011**, *84* (1), 60–64.
161. Liu, Z.; Zhang, A.; Guo, Y.; Dong, C. *Biosens. Bioelectron.* **2014**, *58*, 242–248.
162. Lu, D.; Lin, S.; Wang, L.; Shi, X.; Wang, C.; Zhang, Y. *Electrochim. Acta* **2012**, *85*, 131–138.
163. Fu, L.; Lai, G.; Yu, A. *RSC Adv.* **2015**, *5* (94), 76973–76978.
164. Zhang, Z.; Gu, S.; Ding, Y.; Shen, M.; Jiang, L. *Biosens. Bioelectron.* **2014**, *57*, 239–244.
165. Nag, S.; Duarte, L.; Bertrand, E.; Celton, V.; Castro, M.; Choudhary, V.; Guegan, P.; Feller, J. *J. Mater. Chem. B Biol. Med.* **2014**, *2* (38), 6571–6579.
166. Zhu, G.; Wu, L.; Zhang, X.; Liu, W.; Zhang, X.; Chen, J. *Chem. - A Eur. J.* **2013**, *19*, 6368–6373.
167. Yang, L.; Zhao, H.; Li, Y.; Li, C.-P. *Sensors Actuators B Chem.* **2015**, *207*, 1–8.
168. Zor, E.; Bingol, H.; Ramanaviciene, A.; Ramanavicius, A.; Ersoz, M. *Analyst* **2014**, *140* (1), 313–321.
169. Zhou, J.; Chen, M.; Diao, G. *ACS Appl. Mater. Interfaces* **2013**, *5* (3), 828–836.
170. Sun, Y.; Mao, X.; Luo, L.; Tian, D.; Li, H. *Org. Biomol. Chem.* **2015**, *13* (35), 9294–9299.
171. Mao, X.; Zhao, H.; Luo, L.; Tian, D.; Li, H. *J. Mater. Chem. C* **2015**, *3* (6), 1325–1329.
172. Swathi, R. S.; Sebastian, K. L. *J. Chem. Phys.* **2008**, *129*, 054703.
173. Swathi, R. S.; Sebastian, K. L. *J. Chem. Phys.* **2009**, *130*, 086101.
174. Wei, W.; Xu, C.; Ren, J.; Xu, B.; Qu, X. *Chem. Commun. (Camb)*. **2012**, *48* (9), 1284–1286.
175. Mao, X.; Tian, D.; Li, H. *Chem. Commun. (Camb)*. **2012**, *48* (40), 4851–4853.
176. Yang, L.; Zhao, H.; Li, Y.; Ran, X.; Deng, G.; Xie, X.; Li, C.-P. *ACS Appl. Mater. Interfaces* **2015**, *7* (48), 26557–26565.
177. Mao, X.; Su, H.; Tian, D.; Li, H.; Yang, R. *ACS Appl. Mater. Interfaces* **2013**, *5* (3), 592–597.
178. Mohanty, S. P. *IEEE Potentials* **2015**, *25* (APRIL 2006), 35–40.
179. Zhu, N.; Han, S.; Gan, S.; Ulstrup, J.; Chi, Q. *Adv. Funct. Mater.* **2013**, *23* (42), 5297–5306.

180. Konkena, B.; Vasudevan, S. *Langmuir* **2012**, *28* (34), 12432–12437.
181. Monošík, R.; Stredánský, M.; Šturdík, E. *Acta Chim. Slovaca* **2012**, *5* (1), 109–120.
182. Lu, L.-M.; Qiu, X.-L.; Zhang, X.-B.; Shen, G.-L.; Tan, W.; Yu, R.-Q. *Biosens. Bioelectron.* **2013**, *45*, 102–107.
183. Wang, G.; Shen, X.; Wang, B.; Yao, J.; Park, J. *Carbon N. Y.* **2009**, *47* (5), 1359–1364.
184. Freeman, R.; Finder, T.; Bahshi, L.; Willner, I. *Nano Lett.* **2009**, *9* (5), 2073–2076.
185. Sun, C.; Walker, K. L.; Wakefield, D. L.; Dichtel, W. R. *Chem. Mater.* **2015**, *27* (12), 4499–4504.
186. Palanisamy, S.; Devasenathipathy, R.; Chen, S.-M.; Ajmal Ali, M.; Karuppiah, C.; Balakumar, V.; Prakash, P.; Elshikh, M. S.; Al-Hemaid, F. M. a. *Electroanalysis* **2015**, *27* (10), 2412–2420.
187. Zhao, H.; Ji, X.; Wang, B.; Wang, N.; Li, X.; Ni, R.; Ren, J. *Biosens. Bioelectron.* **2015**, *65*, 23–30.
188. Wei, H.; Wang, E. *Chem. Soc. Rev.* **2013**, *42* (14), 6060.
189. Lin, Y.; Ren, J.; Qu, X. *Acc Chem Res* **2014**, *47* (4), 1097–1105.
190. Guo, Y.; Guo, S.; Ren, J.; Zhai, Y.; Dong, S.; Wang, E. *ACS Nano* **2010**, *4* (7), 4001–4010.
191. Liu, J.; Leng, X.; Xiao, Y.; Hu, C.; Fu, L. *Nanoscale* **2015**, *7* (28), 11922–11927.
192. Agnihotri, N.; Chowdhury, A. D.; De, A. *Biosens. Bioelectron.* **2015**, *63*, 212–217.
193. Yang, L.; Zhao, H.; Fan, S.; Zhao, G.; Ran, X.; Li, C.-P. *RSC Adv.* **2015**, *5* (79), 64146–64155.
194. Mondal, A.; Jana, N. R. *Chem. Commun.* **2012**, *48* (58), 7316.
195. Gao, J.; Guo, Z.; Su, F.; Gao, L.; Pang, X.; Cao, W.; Du, B.; Wei, Q. *Biosens. Bioelectron.* **2015**, *63*, 465–471.
196. Xue, Q.; Liu, Z.; Guo, Y.; Guo, S. *Biosens. Bioelectron.* **2015**, *68*, 429–436.
197. Yang, Y.; Gao, F.; Cai, X.; Yuan, X.; He, S.; Gao, F.; Guo, H.; Wang, Q. *Biosens. Bioelectron.* **2015**, *74*, 447–453.
198. Zhuo, Y.; Zhao, M.; Qiu, W.-J.; Gui, G.-F.; Chai, Y.-Q.; Yuan, R. *J. Electroanal. Chem.* **2013**, *709* (0), 106–110.
199. Peng, K.; Zhao, H.; Wu, X.; Yuan, Y.; Yuan, R. *Sensors Actuators, B Chem.* **2012**, *169*, 88–95.